THE GEOLOGICAL SOCIETY OF AMERICA®

Contribution of an Eastern Indochina-derived fragment to the formation of island arc systems in the Philippine Mobile Belt

Lin Gong[1,2], Pete Hollings[3], Yu Zhang[4], Jing Tian[1,2], Dengfeng Li[5], Al Emil Berador[6], and Huayong Chen[1,7,†]

[1]*Key Laboratory of Mineralogy and Metallogeny, Guangzhou Institute of Geochemistry, Chinese Academy of Sciences, Guangzhou 510640, China*

[2]*University of Chinese Academy of Sciences, Beijing 100049, China*

[3]*Department of Geology, Lakehead University, 955 Oliver Road, Thunder Bay, Ontario P7B 5E1, Canada*

[4]*School of Geosciences and Info-Physics, Central South University, Changsha 410083, China*

[5]*Key Laboratory of Marine Resources and Coastal Engineering, Sun Yat-sen University, Guangzhou 510472, China*

[6]*Regional Office 7, Mines & Geosciences Bureau, Philippine Department of Environment & Natural Resources, 6014 Mandaue, Philippines*

[7]*Guangdong Provincial Key Laboratory of Mineral Physics and Materials, Guangzhou 510640, China*

ABSTRACT

The Philippine Mobile Belt is a complex plate boundary with multiple terranes in Southeast Asia, yet its early tectonic evolution is still not fully understood due to a scarcity of solid evidence. Here we report new whole rock geochemical, Sr-Nd isotopic, and zircon U-Pb-Hf isotopic data for Cretaceous-Miocene arc magmatic rocks from the Cebu and Bohol Islands, Philippine Mobile Belt. Bulk geochemical data display arc affinities with enriched large ion lithophile elements (e.g., Sr and Ba) and depleted high field strength elements (e.g., Nb, Ta, and Ti). The high positive $\varepsilon_{Nd}(t)$ (+4.6 to +9.1) values and low initial $^{87}Sr/^{86}Sr$ ratios (0.7032–0.7048) suggest that these igneous rocks were generated by partial melting of mantle wedge in an arc setting. U-Pb dating of zircons revealed Cretaceous (ca. 120–90 Ma), middle Eocene to early Oligocene (ca. 43–30 Ma), and middle Miocene (ca. 14 Ma) crystallization ages for the arc magmatism with abundant Permian-Triassic zircon xenocrysts clustering at ca. 250 Ma. The Permian-Triassic grains show dominantly negative $\varepsilon_{Hf}(t)$ values ranging from −16.2 to −6.6, which are similar to those of coeval rocks in Eastern Indochina. Combined with previous paleomagnetic studies, we propose that an Eastern Indochina-derived continental fragment was involved during the formation of arcs in the Cebu and Bohol Islands, which highlights the potential contribution of ancient continental materials in the formation of intra-oceanic arcs. This scenario does not support the previously proposed model that the Cretaceous arc in the Philippine Mobile Belt formed in the northern margin of the proto-Philippine Sea Plate and Australian margin.

INTRODUCTION

The Philippine Mobile Belt is a complex tectonic domain with multiple terranes (Rangin, 1991; Pubellier et al., 2003; Hall, 2012) situated at the boundary of the Philippine Sea Plate, the Indo-Australian Plate, and the Eurasian Plate (Fig. 1A). Arc magmatism in the Philippine Mobile Belt commenced in the Early Cretaceous (Deng et al., 2015; Zhang et al., 2020b), yet current oceanic basins surrounding the Philippine Mobile Belt were formed in the Cenozoic. Hence, previous studies have proposed that ancient subduction of the Paleo-Pacific or Pacific Plate beneath the cryptic proto-Philippine Sea Plate on the northern margin of the Australian Plate could account for the formation of the Early Cretaceous arc within the Philippine Mobile Belt (Pubellier et al., 2003; Deng et al., 2015; Dimalanta et al., 2020). This model is largely based on the assumption that the Huatung Basin (Fig. 1B) and the Mesozoic ophiolitic rocks in the Philippine Mobile Belt were remnants of the proto-Philippine Sea Plate and the geochemical and age similarities between the Mesozoic arc rocks in the West Philippine Basin and those in the Philippine Mobile Belt (Hall et al., 1995; Deng et al., 2015; Lallemand, 2016; Dimalanta et al., 2020). Alternatively, it has been suggested that crustal fragments rifted from the Eurasian continental margin were incorporated into the western part of the Philippine Mobile Belt based on the presence of metamorphic basements with continental affinity (Rangin et al., 1990; Rangin, 1991; Yumul et al., 2020a, 2020b). This implies that the incipient Philippine arc system was possibly formed by subduction of the Pacific Plate beneath oceanic basins in the margin of Eurasian Plate (Holloway, 1982). The existence of the proto-Philippine Sea Plate and early evolution of the Philippine arc within the Philippine Mobile Belt are therefore still subject to debate. This limits our understanding of the tectonic evolution of Southeast Asia (Hall, 2012; Zahirovic et al., 2014) and crustal growth processes in the Philippines.

Paleomagnetism should provide critical evidence for testing these different models, but there is considerable variation in the interpretations of the paleomagnetic data (mainly Cenozoic) within the Philippine Mobile Belt regarding the paleolatitude (northern hemisphere or southern hemisphere) and plate motion (Fuller et al., 1983; McCabe et al., 1987; Fuller et al., 1989; Fuller et al., 1991; Queano et al., 2007; Balmater et al., 2015). These discrepancies are likely due to tectonic complexity, the limited amount of data, and significant uncertainties about the paleolatitude (McCabe et al., 1987; Queano et al., 2007). A recent reinterpretation of paleomagnetic data from Cebu Island in the central Philippines suggests a northern hemisphere paleolatitude during the Cretaceous (Yumul et al., 2020a), which is inconsistent with the Philippine Mobile Belt being derived from the northern margin of Australia (Pubellier et al., 2003; Deng et al., 2015; Dimalanta et al., 2020).

†Corresponding author: huayongchen@gig.ac.cn.

GSA Bulletin; September/October 2021; v. 133; no. 9/10; p. 1979–1995; https://doi.org/10.1130/B35793.1; 11 figures; 1 supplemental file.
published online 21 January 2021

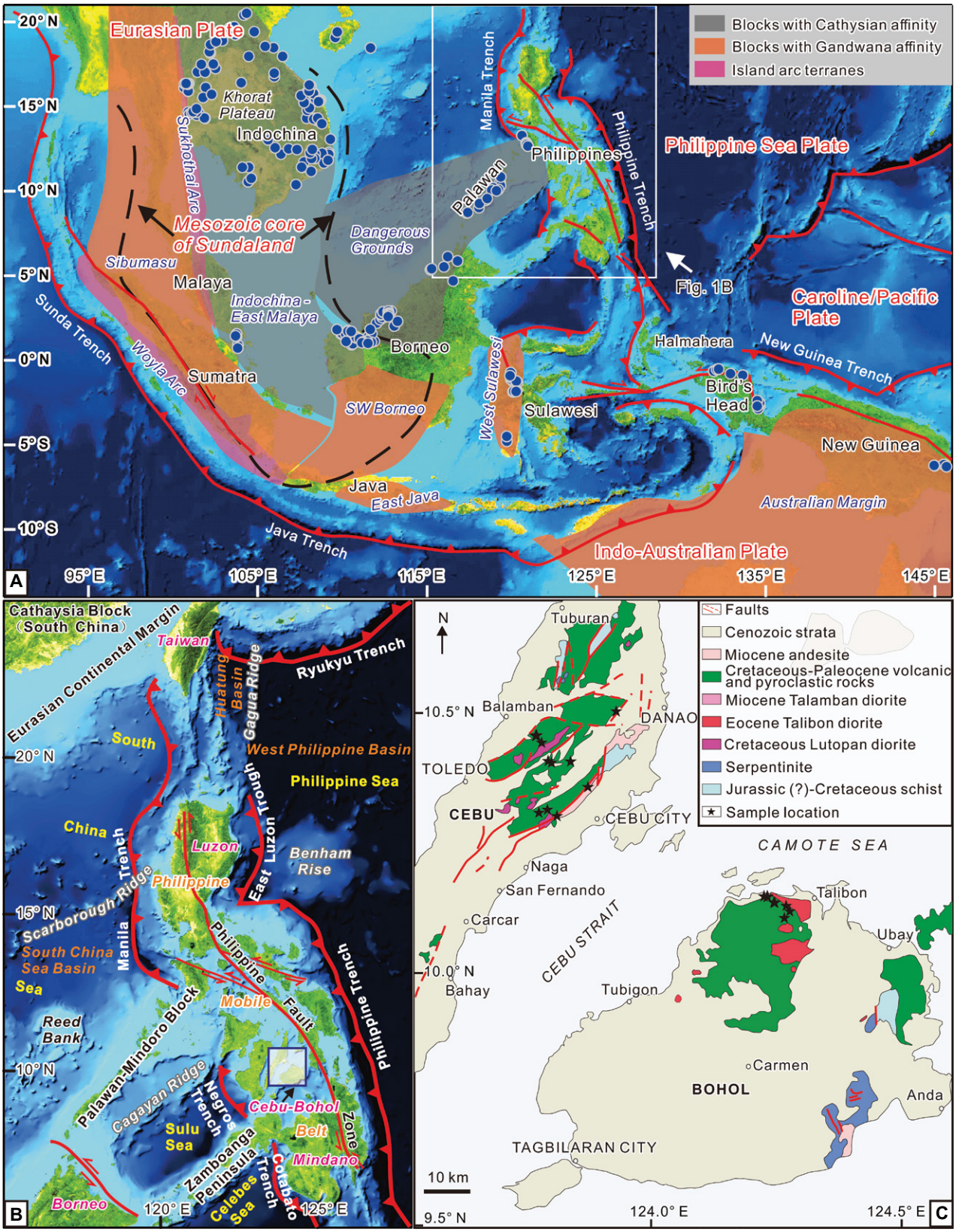

Figure 1. (A) The distribution of major plates, terranes, and fragments in Southeast Asia (modified after Hall, 2017; and Zhang et al., 2020a) is shown with the compiled samples in circle points. The detailed locations, ages, and references for these samples are provided in Table S5 (see footnote 1). (B) Tectonic framework of the Philippine Mobile Belt and its surrounding terranes (modified after Yumul et al., 2008). (C) Schematic geological map of Cebu and Bohol Islands (modified after Aurelio and Peña, 2010).

Zircons incorporated into island arc igneous rocks may provide another window into the origin and nature of their host rocks (Smyth et al., 2007; Buys et al., 2014; Shao et al., 2015; Li et al., 2018; Zhang et al., 2018, 2019). Zircon chemistry may provide crucial additional constraints for tectonic reconstructions, especially for regions with complex tectonics and/or conflicting paleomagnetic data. We present whole rock geochemistry, Sr-Nd isotope, and zircon U-Pb-Hf isotope data for the Early Cretaceous to middle Miocene magmatic rocks of the Cebu and Bohol Islands to investigate the evolution of the Philippine arc within the Philippine Mobile Belt. We document abundant continental zircon xenocrysts (mainly Permian to Triassic) with an Eastern Indochina affinity, which enables us to propose that Eastern Indochina-derived continental materials were involved in the generation of the island arc systems within the Philippine Mobile Belt rather than materials from the Australian margin, as previously speculated (Deschamps and Lallemand, 2002; Pubellier et al., 2003; Deng et al., 2015; Dimalanta et al., 2020).

GEOLOGICAL BACKGROUND

The Philippine Mobile Belt, a product of oblique convergence between the Philippine Sea Plate and the thinned margin of the Eurasian Plate (Rangin et al., 1990; Rangin, 1991), is bounded by oppositely dipping subduction zones (Fig. 1B) and underlain by Jurassic-Cretaceous basement composed of ophiolitic complexes with different origins (Pubellier et al., 2003; Dimalanta et al., 2020; Yumul et al., 2020b), including marginal basins rifted from both the Eurasian and Indo-Australian Plates (Rangin, 1991; Deng et al., 2015; Dimalanta et al., 2020). Arc systems within the Philippine Mobile Belt were mainly formed in the Cretaceous, Eocene, Oligo-Miocene, and Pliocene-Quaternary (Aurelio et al., 2013). The Cretaceous arc is generally thought to have been related to subduction between the Pacific or Paleo-Pacific Plates and the marginal basins (e.g., proto-Philippine Sea Plate) of the Australian Plate (Deschamps and Lallemand, 2002; Pubellier et al., 2003; Zahirovic et al., 2014; Deng et al., 2015). However, an earlier model proposed that the Cretaceous arc in the Philippines resulted from subduction of the Pacific Plate beneath oceanic basins of the Eurasian margin (Holloway, 1982). The Eocene to Miocene arcs within the Philippine Mobile Belt are generally considered to be associated with the subduction of oceanic basins beneath the Philippine Sea Plate (Rangin, 1991; Hall, 2002; Pubellier et al., 2003; Hall, 2012). Subduction ceased when the Philippine Mobile Belt collided with the rifted Eurasian margin (e.g., Palawan block and Zamboanga Peninsula) in the Miocene (Pubellier et al., 2003; Yumul et al., 2004, 2008). The magmatic arc commenced again from the Pliocene to Quaternary due to subduction of the oceanic plates surrounding the Philippine Mobile Belt (Fig. 1B; Aurelio et al., 2013; Dimalanta et al., 2020).

The Cebu and Bohol Islands, located in the central part of the Philippine Mobile Belt, represent an excellent site for studying the origin and evolution of the Philippine arc because they encompass all of the early magmatic arcs of the Philippine Mobile Belt. The oldest arc-related rocks within the Philippine Mobile Belt crop out on Cebu Island (Deng et al., 2015) and consist of Cretaceous basaltic to andesitic volcanic-pyroclastic rocks and dioritic intrusions (Fig. 1C; Deng et al., 2015, 2017; Zhang et al., 2020b). These Cretaceous volcanic rocks were covered or intruded by the middle Miocene andesite and diorite in the east of Cebu Island (Fig. 1C). Only middle Eocene to early Oligocene arc volcanic and intrusive rocks and Miocene andesites are found on Bohol Island (Fig. 1C; Aurelio and Peña, 2010). In addition to the arc magmatic rocks, metamorphic complex consisting of chlorite schist, micaceous schist, and amphibolite schist with ages ranging from Jurassic to Cretaceous are found on Bohol and Cebu Islands (Yumul et al., 2001; Dimalanta et al., 2006). These metamorphic complexes on both islands were formed in subduction-related settings (Yumul et al., 2001; Dimalanta et al., 2006). The sedimentary strata are dominated by middle Eocene to late Pleistocene siliciclastic and carbonate sedimentary units with some Cretaceous sandstone and limestone on Cebu Island (Aurelio and Peña, 2010).

SAMPLES AND METHODS

A total of 19 samples including andesite, basaltic andesite, basalt, and basaltic-andesitic to andesitic volcaniclastic rocks were collected from Cebu and Bohol Islands ranging in age from Cretaceous ($n = 6$), middle Eocene to early Oligocene ($n = 12$), and middle Miocene ($n = 1$). Among these samples, one Cretaceous sample (C9-2), two Paleogene samples (C19-8 and B17), and one middle sample (C24) contain igneous xenoliths, and xenoliths were not involved during the geochemical analysis of these samples. Most of the volcanic rocks are characterized by porphyritic textures with phenocrysts consisting of plagioclase, hornblende, and clinopyroxene in a matrix of fine-grained feldspars, amphibole, pyroxene, Fe-Ti oxide, and aphanitic crystals. Most plagioclase and some clinopyroxene show variable alteration to sericite and amphibole, respectively. The volcaniclastic rocks are mainly composed of plagioclase and amphibole crystal fragments with minor andesite debris. Representative petrographic descriptions and photomicrographs are provided in the Supplemental Materials (Figs. S1-1 to S1-3)[1].

Thirteen least altered samples were analyzed for whole rock major- and trace-element concentrations and Sr-Nd isotopes. The major and trace elements were analyzed at ALS Minerals/ALS Chemex (Guangzhou) Co. Ltd., Guangzhou, China. Major oxide concentrations were measured using a PANalytical Axios X-ray fluorescence spectrometer (XRF) on fused glass beads at 1050–1100 °C with a $Li_2B_4O_7$–$LiBO_2$ flux with analytical precisions generally better than ± 1%. Trace element concentrations were determined by inductively coupled plasma-mass spectrometry (ICP–MS), and the analytical precisions were generally better than ± 5%.

Sr and Nd isotopic analyses were performed on a Neptune Plus multi-collector-inductively coupled plasma-mass spectrometer (MC-ICP-MS) at the Guangzhou Institute of Geochemistry, Chinese Academy of Sciences, Guangzhou, China, using analytical procedures described by Wei et al. (2002) and Liang et al. (2003). Sr and rare earth elements (REE) were separated using cation columns, and Nd fractions were further separated by Di-(2-ethylhexyl) phosphoric acid (HDEHP)-coated Kef columns. The measured isotopic fractionations were corrected to $^{86}Sr/^{88}Sr = 0.1194$ and $^{146}Nd/^{144}Nd = 0.7219$. The measured weighted mean $^{87}Sr/^{86}Sr$ of NBS987 standard material was 0.710247 ± 0.000003 (1σ, $n = 9$), and the measured weighted mean $^{143}Nd/^{144}Nd$ of JNdi-1 standard material was 0.512110 ± 0.000002 (1σ, $n = 8$), and both are within the errors of recommended values (Jochum et al., 2005). To monitor the processes of sample digestion and purification, BHVO-2 was run as an external standard. Two measurements of the BHVO-2 yielded a weighted mean of $^{143}Nd/^{144}Nd = 0.512976 \pm 0.000007$ (1σ), which is within the error of the recommended values (Jochum et al., 2005).

Zircons were separated from 19 volcanic and pyroclastic rocks using conventional magnetic and heavy liquid techniques. Then the selected zircons were mounted on standard epoxy casts and imaged by cathodoluminescence (CL)

[1]Supplemental Material. Figures S1–S7 and Table S1–S5. Please visit https://doi.org/10.1130/GSAB.S.13394207 to access the supplemental material, and contact editing@geosociety.org with any questions.

using a TESCAN MIRA3 field emission scanning electron microscope at the Testing Center, Tuoyan Technology Co., Ltd., Guangzhou, China. In situ U-Pb dating and trace element analyses were carried out on the zircon grains using an LA-ICP-MS system at Nanjing FocuMS Technology Co. Ltd. and the Key Laboratory of Marine Resources and Coastal Engineering, Sun Yat-sen University (SYU), Guangzhou, China. The SYU analytical details can be found in Fu et al. (2015). Laser sampling of zircon was conducted using a Teledyne Cetac Technologies Analyte Excite laser ablation system with laser beam energy of 6.0 J/cm^2, and ion-signal intensities were acquired using Agilent Technologies' 7700× quadrupole ICP-MS at Nanjing FocuMS Technology Co., Ltd. Laser ablation spots were 35 μm in diameter with an ablation rate of 8 Hz and with typical data acquisition of 40 s for the sample and 20 s for the background. Helium was used as the carrier gas to efficiently transport aerosol to ICP-MS.

Zircon 91500 was used as an external standard to correct instrumental mass discrimination and elemental fractionation during ablation. Every eight sample analyses were followed by analysis of two 91500 zircon standards. Zircon standard GJ-1 and Plešovice were used as quality control during U-Pb dating. Pb abundance of zircon was externally calibrated against NIST SRM 610 with Si used for internal standardization and Zr as an internal standard for the other trace elements. The ICPMSDataCal software (Liu et al., 2010) was used for raw data reduction. The dating results of zircon standard Plešoviceare and 91500 were 338.5 ± 0.8 (1σ; n = 31; Fig. S2A; see footnote 1) and 1062.4 ± 2.2 (1σ; n = 70; Fig. S2B) at SYU, respectively. Zircon standard Plešoviceare, 91500 and GJ-1 at Nanjing FocuMS Technology Co., Ltd., yielded weighted mean ages of 339.1 ± 0.7 (1σ; n = 27; Fig. S2C), 1062.2 ± 1.3 (1σ; n = 92; Fig. S2D), and 602.2 ± 1.0 (1σ; n = 46; Fig. S2E), respectively. These ages are consistent with recommended values within 1σ (Wiedenbeck et al., 1995; Jackson et al., 2004; Sláma et al., 2008).

Zircon Hf isotopic ratios were measured using a Nu Instruments Nu Plasma II MC-ICP-MS combined with a Teledyne Cetac Technologies Analyte Excite laser ablation system at Nanjing FocuMS Technology Co., Ltd. The laser ablation energy density used was 8.0 J/cm^2. Each acquisition incorporated 20 s background followed by 40 s from the sample with a spot diameter of 50 μm and 9 Hz repetition rate. Helium was used as the carrier gas to efficiently transport aerosol out of the ablation cell. Standard zircons (including GJ-1, 91500, Plešovice, Mud Tank, and Penglai) were used as quality control after every five unknown samples. Analyses of the zircon standard 91500, GJ-1, Mud Tank, Plešovice, and Penglai yielded weighted mean $^{176}Hf/^{177}Hf$ ratios of 0.2823085 ± 0.0000029 (1σ; n = 12; Fig. S2F), 0.2820102 ± 0.0000021 (1σ; n = 21; Fig. S2G), 0.2825169 ± 0.0000021 (1σ; n = 12; Fig. S2H), 0.2824809 ± 0.0000018 (1σ; n = 14; Fig. S2I), and 0.2829080 ± 0.0000029 (1σ; n = 12; Fig. S2J), respectively, consistent with the recommended values within 1σ (Sláma et al., 2008; Yuan et al., 2008; Li et al., 2010).

RESULTS

Whole Rock Geochemistry and Sr-Nd Isotopes

The bulk geochemistry data are provided in Table S1 (see footnote 1). They display relatively low SiO_2 (52–61 wt%, normalized to 100% anhydrous and the same hereafter), low to middle K_2O (0.04–1.86 wt%), high Na_2O (1.23–7.01 wt%) contents, with variable loss on ignition (0.50–6.66 wt%), plotting in the basalt to andesite fields on the Nb/Y-Zr/Ti diagram (Fig. 2A; after Pearce, 2014) with tholeiitic to calc-alkaline affinities (Fig. 2B; after Peccerillo and Taylor, 1976). The Al_2O_3 and CaO contents range from 10–19 wt% and 3–14 wt%, respectively, indicating a metaluminous affinity with an aluminum saturation index (A/CNK = molar $Al_2O_3/[CaO + Na_2O + K_2O]$) of 0.37–1.00. The samples have variable MgO (3–12 wt%) and Fe_2O_{3T} (5–12 wt%) concentrations with relatively high Mg# [molar Mg/(Mg + Fe)] ranging from 42 to 71.

The samples have low total REEs (30.3–194.1 ppm) with slightly negative Eu anomalies (Figs. 3A and 3C; Eu/Eu* = 0.82–1.08). The Cretaceous and middle Miocene samples are light REE (LREE) enriched relative to their heavy REE (HREE) (Fig. 3A; La_N/Yb_N = 2.2–20.2; normalized to the chondrite values from Sun and McDonough [1989]), whereas the

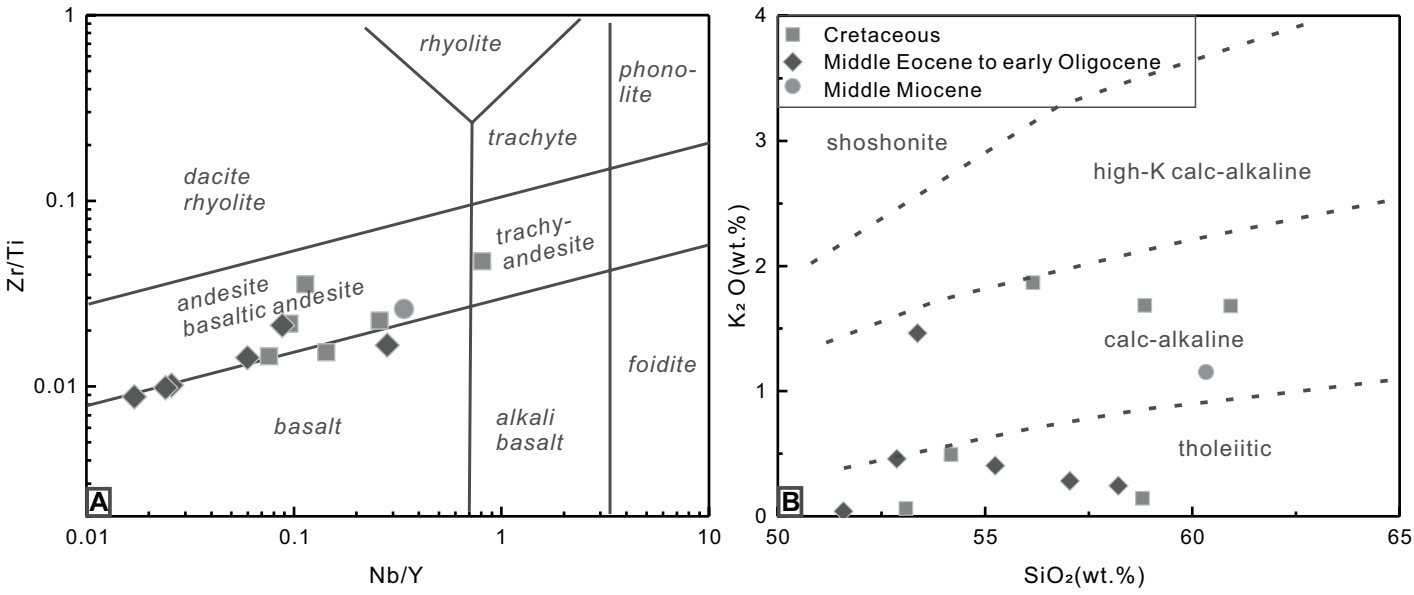

Figure 2. (A) Immobile element TAS (total alkali/silica) proxy diagram is shown (after Pearce, 2014). (B) K_2O versus SiO_2 diagram (after Peccerillo and Taylor, 1976) for igneous rocks from Cebu and Bohol Islands.

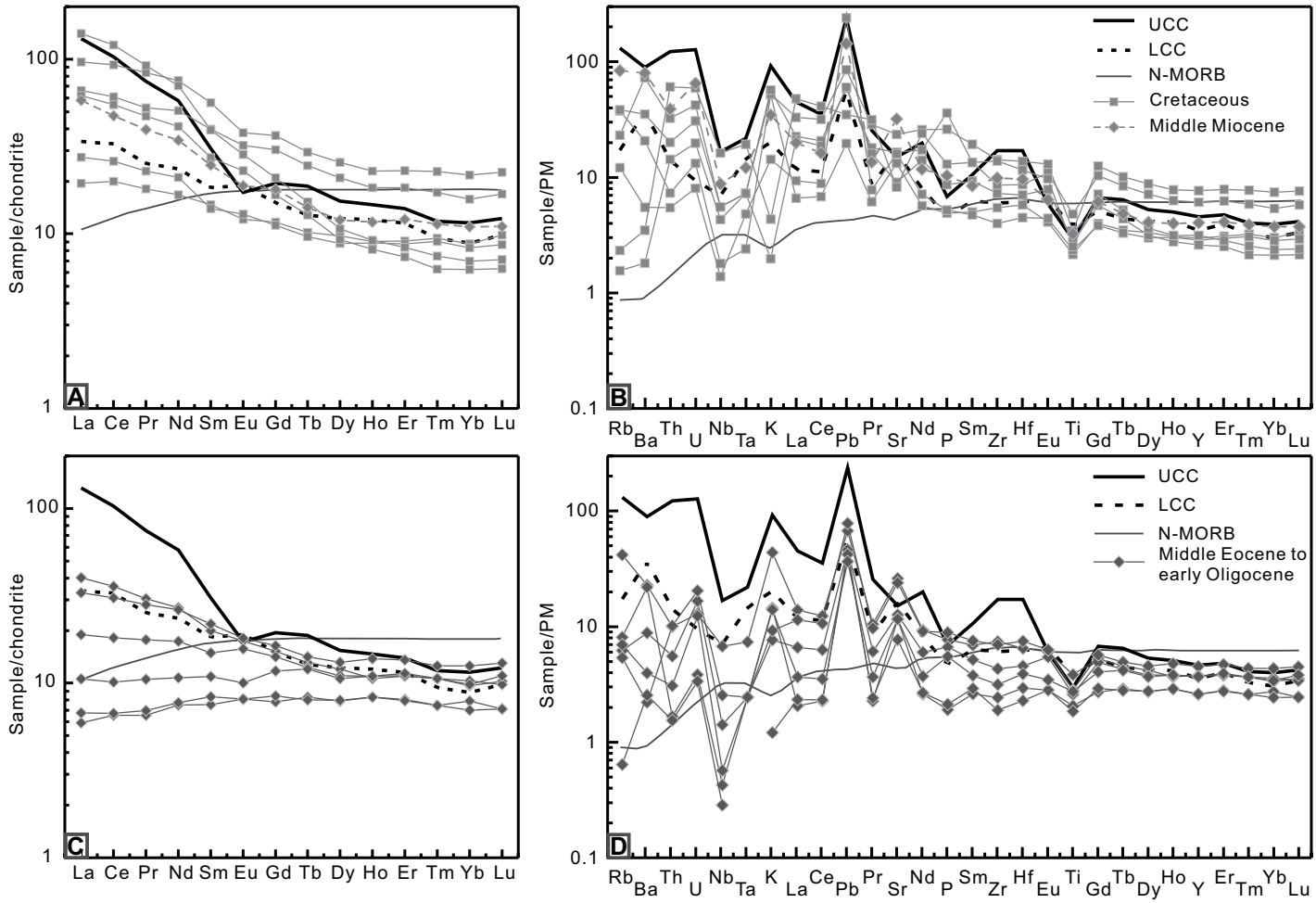

Figure 3. (A, B) Chondrite-normalized rare earth element (REE) pattern and primary mantle-normalized, multi-element diagram for the Cretaceous and middle Miocene igneous rocks in this study is shown. (C, D) Chondrite-normalized REE pattern and primary mantle-normalized, multi-element diagram for the middle Eocene to early Oligocene igneous rocks in this study. Chondrite, primary mantle (PM), and normal mid-oceanic-ridge basalt (N-MORB) compositions are from Sun and McDonough (1989), and upper and lower continental crust (UCC and LCC) compositions are from Rudnick and Gao (2003).

middle Eocene to early Oligocene samples display flat to LREE-enriched patterns (Fig. 3C; $La_N/Yb_N = 0.8–4.2$). The multi-element variation diagrams show that all samples have an arc affinity characterized by depletion in high field strength elements (HFSEs; e.g., Nb, Ta, and Ti) and large ion lithophile elements (LILE) and Pb enrichment (Figs. 3B and 3D; Rudnick and Gao, 2003; Jagoutz and Kelemen, 2015). Generally, the trace element compositions for the Cretaceous and middle Miocene samples are similar to those of lower to upper continental crust (Figs. 3A and 3C; Rudnick and Gao, 2003). Comparatively, the middle Eocene to early Oligocene samples have more depleted trace elements contents, with most of their trace elements more depleted than those of lower continental crust (Figs. 3B and 3D; Sun and McDonough, 1989; Rudnick and Gao, 2003). All samples exhibit depleted isotopic signatures with high and moderately variable values of $\varepsilon_{Nd}(t)$ (+9.1 to +4.6) and low initial $^{87}Sr/^{86}Sr$ ratios (0.7032–0.7048) (Table S1).

Zircon U-Pb Ages

All of the concordant (≤10% discordance) zircon U-Pb isotopic data are provided in Table S2 (see footnote 1) and trace element data in Table S3. Representative CL images of the dated zircons are presented in Figure 4 and Figure S3 with their corresponding ages and $\varepsilon_{Hf}(t)$ values. Most of the zircons are between 50 μm and 200 μm in length and euhedral to subhedral with several sub-rounded grains. Most grains exhibit oscillatory magmatic zoning, and some have a resorbed dark core with a light-colored rim in CL images (Fig. S3). For grains with core-rim textures, all analyses were performed in the core domain due to the thin rims. The Th and U concentrations vary from 8–8427 ppm and 24–3115 ppm, respectively, with Th/U ratios mostly ranging from 0.1 to 3 (Fig. 5A). Most zircons are enriched in HREEs relative to LREEs with positive Ce and negative Eu anomalies (Fig. 5B). Nearly all zircons high U/Yb ratios are consistent with zircons derived from island and continental arcs (Fig. 5C; Grimes et al., 2007). The interior structure, crystal morphology, and Th/U ratios collectively indicate that the zircons are predominantly magmatic in origin (Figs. 4 and 5A; Hoskin and Schaltegger, 2003; Wu and Zheng, 2004).

A total of 23 measurements were carried out on zircons from the pyroxene andesite sample C9-2, yielding 16 concordant ages from 137 Ma to 107 Ma. The five youngest

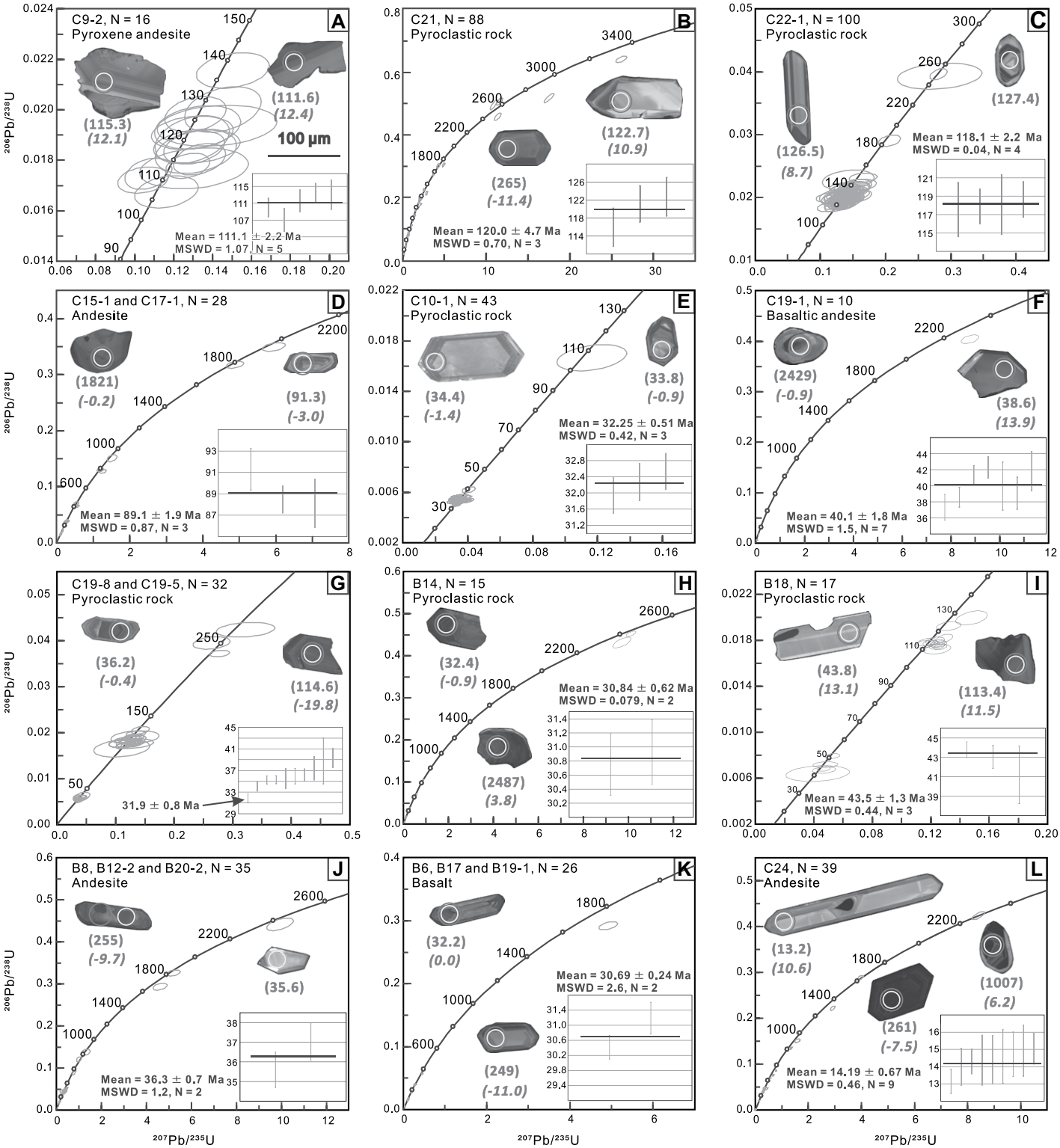

Figure 4. U-Pb concordia diagrams, weighted mean ages, and representative cathodoluminescence (CL) images are shown for zircons with their corresponding U-Pb ages and $\varepsilon_{Hf}(t)$ values (in italics) of igneous rocks from the Cebu and Bohol Islands, Philippine Mobile Belt. N is the number of measurements. MSWD—mean square of weighted deviates.

grains defined a weighted mean $^{206}Pb/^{238}U$ age of 111.1 ± 2.2 Ma (1 standard deviation [1σ]; mean square of weighted deviates [MSWD] = 1.1; Fig. 4A), representing the crystallization age for the magmatic protolith. Ninety-six zircon grains were analyzed from pyroclastic rock sample C21, yielding 88 concordant ages of 3435–116 Ma, with a crystallization age of 120.0 ± 4.7 Ma (1σ; MSWD = 0.47)

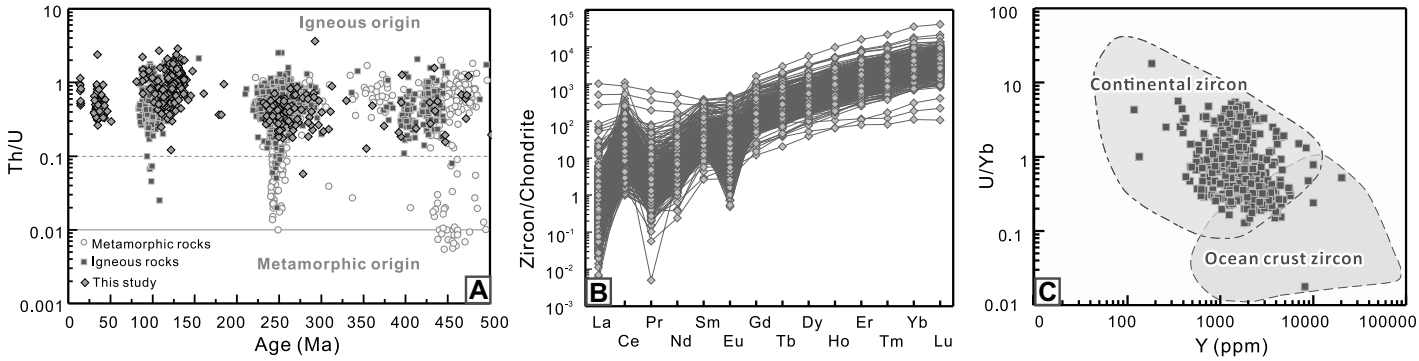

Figure 5. (A) The Th/U ratio of zircon grains with different ages is shown. The zircon grains with Th/U < 0.01 are conventionally considered to be metamorphic in origin, whereas magmatic zircon rarely have Th/U ratios lower than 0.1 (Hoskin and Schaltegger, 2003; Wu and Zheng, 2004). Data for metamorphic and igneous rocks are compiled from the eastern margin of the Indochina block (see Table S5 [see footnote 1]; Carter and Moss, 1999; Usuki et al., 2009; Shellnutt et al., 2013; Burrett et al., 2014; Tran et al., 2014; Hieu et al., 2015; Shi et al., 2015; Arboit et al., 2016; Owada et al., 2016; Wang et al., 2016; Hou et al., 2019; Nguyen, 2019; Bui et al., 2020). (B). Chondrite-normalized rare earth element (REE) pattern of zircons from igneous rocks of the Cebu and Bohol Islands. Normalizing values are from Sun and McDonough (1989). (C) Discrimination diagram for zircon origin (after Grimes et al., 2007).

using the three youngest grains (Fig. 4B). Abundant xenocrystic/inherited zircons were identified from this sample and primarily ranged from 303 Ma to 239 Ma ($N = 34$; Fig. S4 and Table S2; see footnote 1). One hundred concordant U-Pb ages were obtained on 107 analyzed zircon crystals from pyroclastic rock sample C22-1, including two Permian-Triassic grains (250.3 ± 3.7 Ma and 248.7 ± 8.6 Ma), one Jurassic grain (184.4 ± 3.7 Ma), and the remaining crystals varied from 147 Ma to 117 Ma. The youngest population gave a weighted mean age of 118.1 ± 2.2 Ma (1σ; MSWD = 0.04; $N = 4$; Fig. 4C), which is assumed to be the crystallization age of the parental magma. From andesite sample C20, only 10 zircon grains were recovered and seven concordant ages of 1343–108 Ma were identified (Table S2). The youngest grain (107.5 ± 1.6 Ma) was estimated to represent the maximum crystallization age of this sample. These crystallization ages are consistent with previous zircon U-Pb dating results from andesite (126.2 ± 2.4 Ma; Deng et al., 2015), pyroclastic rock (118.5 ± 1.2 Ma; Deng et al., 2015), and diorite (108.5 ± 1.6 Ma; Zhang et al., 2020b) from Cebu Island. In total, 33 zircons were analyzed from two andesite samples, C15-1 and C17-1, with 28 concordant ages varying from 2005 Ma to 88 Ma. The maximal crystallization or eruption age was estimated to be 89.1 ± 1.4 Ma (1σ; MSWD = 0.87; $N = 3$; Fig. 4D) based on the youngest population. This age is identical to previous Late Cretaceous fossil ages from sedimentary interbeds in the volcanic sequence (Aurelio and Peña, 2010).

Among the three pyroclastic rock samples (C10-1, C19-5, and C19-8) from Cebu Island, 43 concordant ages were obtained from 49 analyzed zircon grains from sample C10-1. Except for one zircon xenocryst (106.5 ± 4.3 Ma), the remaining grains yielded ages of 40–32 Ma with a weighted mean $^{206}Pb/^{238}U$ age of 32.4 ± 0.5 Ma (1σ; MSWD = 0.42; $N = 3$; Fig. 4E), which is interpreted to be the crystallization age. In addition, pyroclastic rock samples C19-5 and C19-8 were possible from the same eruptive sequence based on the field observations and their similarly youngest zircon populations. These two samples yielded 32 concordant ages from 49 measured zircon crystals and showed age populations at 267–236 Ma, 131–106 Ma, and 39–32 Ma. The youngest single grain age (31.9 ± 0.8 Ma; Fig. 4G) likely represents the crystallization age of the magmatic protolith. A total of 17 analyses were performed on zircons, and 10 concordant ages were obtained from andesite sample C19-1. Except for three xenocrysts (2429 Ma, 846 Ma, and 110 Ma), the remaining homogeneous grains yielded a weighted mean $^{206}Pb/^{238}U$ age of 40.1 ± 1.8 Ma (1σ; MSWD = 1.5; $N = 7$; Fig. 4F), which is interpreted to be the crystallization age. These results indicate that some igneous rocks from Cebu Island previously mapped as Cretaceous (Aurelio and Peña, 2010) were formed in the middle Eocene to early Oligocene. On Bohol Island, two pyroclastic rock samples (B14 and B18) were collected for dating. Sixteen U-Pb dates were determined from sample B14, with 15 being concordant and ranging from 2487 Ma to 31 Ma. The youngest grains yielded a weighted mean $^{206}Pb/^{238}U$ age of 30.8 ± 0.6 Ma (1σ; MSWD = 0.08; $N = 2$; Fig. 4H). With the exception of 127–110 Ma and 51–46 Ma xenocrystic/inherited zircons ($N = 12$ and $N = 2$, respectively), the remaining three zircons from sample B18 gave a weighted mean $^{206}Pb/^{238}U$ age of 42.5 ± 1.3 Ma (1σ; MSWD = 0.44; Fig. 4I). Both mean ages can be interpreted as crystallization ages of their parental magmas. Based on the similar mineral assemblages and field observations, three andesite samples (B8, B12-2, and B20-2) from Bohol Island should be the same lithofacies. In total, 35 concordant ages were obtained from 38 analyses from these three samples, with ages of 2487–1862 Ma, 834–736 Ma, 548 Ma, 395–311 Ma, 291–235 Ma, 142–103 Ma, and 43–36 Ma. The youngest two zircons yielded a weighted mean $^{206}Pb/^{238}U$ age of 36.3 ± 0.7 Ma (1σ; MSWD = 1.2; Fig. 4J). Similarly, three basalt samples (B6, B17, and B19-1) from Bohol Island have comparable mineral assemblages and were likely to form a common volcanic layer. A total of 27 zircon U-Pb measurements from these samples yielded 26 concordant ages of 1987 Ma, 396–361 Ma, 251–249 Ma, 181–179 Ma, 119–89 Ma, and 38–30 Ma with a weighted mean $^{206}Pb/^{238}U$ age of 30.7 ± 0.2 Ma (1σ; MSWD = 2.6; $N = 2$; Fig. 4K). These two weighted mean ages represent the crystallization ages of their magmatic protolith, and the dating results are also consistent with the cross-cutting relationship that the andesites were presented as xenoliths in basalts (Fig. S1-2C). A total of 50 zircons were selected for dating from andesite sample C24 from Cebu Island, yielding 39 concordant ages. The xenocrystic/inherited zircons were identified to be 2445–2265 Ma, 1783–1350 Ma, 1007–820 Ma, 532–392 Ma, 309–239 Ma, and 131 Ma in age ($N = 30$). The remaining nine grains yielded a weighted mean $^{206}Pb/^{238}U$ age of 14.2 ± 0.7 Ma (1σ; MSWD = 0.46; Fig. 4L), which represents the best estimate of the eruption age.

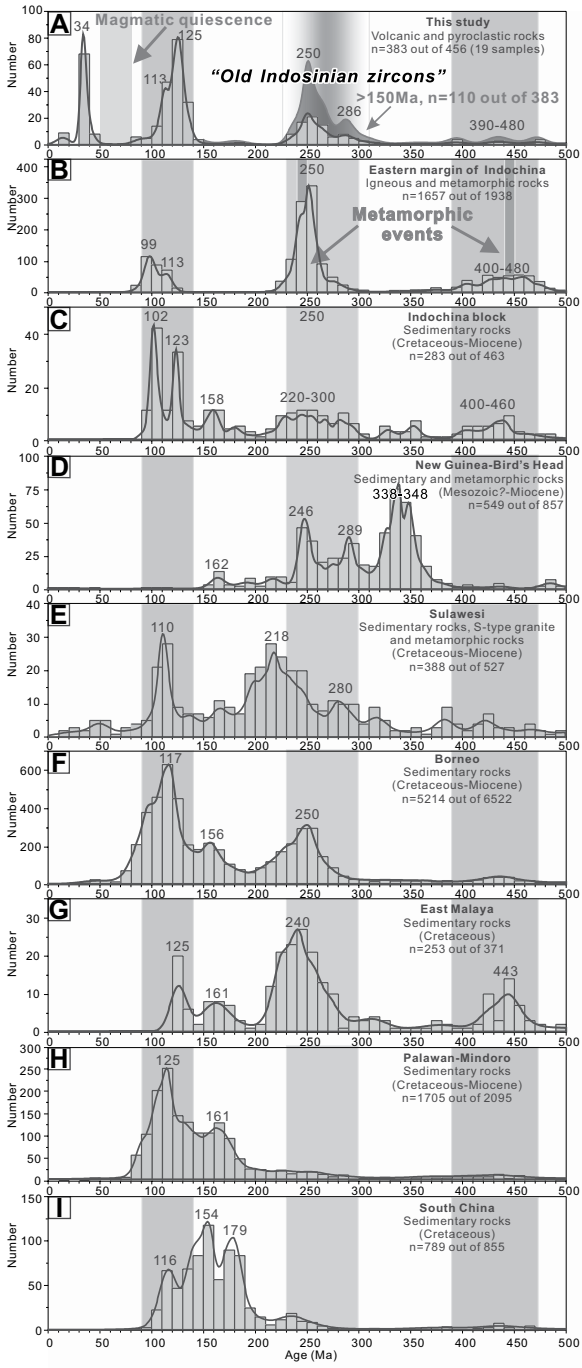

Figure 6. (A) U-Pb age spectra of zircons from igneous rocks of the Cebu and Bohol Islands are shown. (B) Histogram and relative probability density diagram of compiled zircons from igneous rocks and metamorphic rocks in the eastern margin of the Indochina terrane (Usuki et al., 2009; Shellnutt et al., 2013; Tran et al., 2014; Hieu et al., 2015; Shi et al., 2015; Hieu et al., 2016; Owada et al., 2016; Wang et al., 2016; Hou et al., 2019; Nguyen, 2019; Bui et al., 2020; Minh et al., 2020). (C) Histogram and relative probability density diagram of compiled detrital zircons for Cretaceous to Miocene sedimentary rocks of the Indochina terrane (Carter and Moss, 1999; Burrett et al., 2014; Hennig et al., 2018). (D) Histogram and relative probability density diagram of compiled detrital or inherited zircons from possibly Mesozoic to Miocene sedimentary and metamorphic rocks of New Guinea-Bird's Head Peninsula (Van Wyck and Williams, 2002; Webb et al., 2019; White et al., 2019). (E) Histogram and relative probability density diagram of compiled detrital or inherited zircons from sedimentary rocks, metamorphic rocks, and S-type granite in Sulawesi (Hennig et al., 2016; Jaya et al., 2017). (F) Histogram and relative probability density diagram of compiled detrital zircons from Cretaceous to Miocene sedimentary rocks in Borneo (van Hattum et al., 2006; Breitfeld et al., 2017; Galin et al., 2017; Breitfeld and Hall, 2018; Hennig-Breitfeld et al., 2019). (G) Histogram and relative probability density diagram of compiled detrital zircons from Cretaceous sedimentary rocks in East Malaya (Dodd et al., 2019). (H) Histogram and relative probability density diagram of compiled detrital zircons from Cretaceous to Miocene sedimentary rocks in Palawan-Mindoro (Suggate et al., 2014; Shao et al., 2017; Yan et al., 2018). (I) Histogram and relative probability density diagram of compiled detrital zircons from Cretaceous sedimentary rocks of the south margin of South China (Jiang et al., 2015; Shao et al., 2017).

The detailed age distribution of each sample is provided in Figure S4, and all of these samples can be categorized into three groups based on their crystallization or maximum eruption age into the Cretaceous (ca. 120–90 Ma), middle Eocene to early Oligocene (ca. 43–30 Ma), and middle Miocene (ca. 14 Ma). The inherited/xenocrystic zircon age distributions from each group are similar to each other (Fig. S5). In summary, the dominant age populations (Fig. 6A) are middle Miocene (peaking at ca. 14 Ma), middle Eocene to early Oligocene (ca. 46–30 Ma with a peak at ca. 34 Ma), Cretaceous (ca. 147–88 Ma with peaks at 125 Ma and 113 Ma), and Permian-Triassic (ca. 300–232 Ma with peaks at ca. 286 Ma and 250 Ma). There are also some minor Ordovician-Devonian (ca. 480–390 Ma), Meso- to Neoproterozoic (ca. 1.3–0.7 Ga), and Archean (ca. 2.5 Ga) peaks, which will not be discussed further due to the limited numbers for these ages.

Hf Isotopes

Lutetium-Hf isotopic analyses were conducted on 179 dated zircons, and results are presented in Table S4 (see footnote 1; Blichert-Toft and Albarède, 1997; Griffin et al., 2000, 2002; Söderlund et al., 2004) and Figure 7. Most Permian-Triassic zircons have negative $\varepsilon_{Hf}(t)$ values of −16.2 to −6.6 and crustal model ages (T_{DM}^{C}) of 2.2–1.7 Ga. The Hf isotopic compositions of the Cretaceous grains can be categorized into three groups. One group with ca. 113–111 Ma ages ($N = 5$) displays high negative $\varepsilon_{Hf}(t)$ values of −25.2 to −16.2 and crustal model ages (T_{DM}^{C}) of 2.7–2.2 Ga. The second group ($N = 12$), with ages of ca. 126–81 Ma, is characterized by negative to weakly positive $\varepsilon_{Hf}(t)$ values of −4.9 to +2.8 with crustal model ages (T_{DM}^{C}) of 1.5–1.0 Ga. The third group ($N = 40$), with ages varying from 138 Ma to 109 Ma, shows high positive $\varepsilon_{Hf}(t)$ values of +8.2 to +14.5 and mantle model ages (T_{DM}) of 478–193 Ma. Two different populations of Hf isotopic composition are identified from the Paleogene zircons: one population (46–37 Ma; $N = 7$) with high positive $\varepsilon_{Hf}(t)$ values of +13.1 to +16.0 and mantle model ages (T_{DM}) of 198–74 Ma and the other population (36–32 Ma; $N = 22$) with $\varepsilon_{Hf}(t)$ values of −1.7 to +0.7 with crustal model ages (T_{DM}^{C}) of 1.2–1.0 Ga. All of the middle Miocene zircons exhibit high positive $\varepsilon_{Hf}(t)$ values ranging from +10.6 to +15.0 with mantle model ages (T_{DM}) of 286–93 Ma.

DISCUSSION

Petrogenesis and Magma Sources

The igneous samples collected in this study have variable and high loss on ignition (0.55–6.66 wt%) values, suggesting various degrees of hydrothermal alteration. Therefore, it is necessary to evaluate whether the mobile elements such as LILEs have been remobilized during post-magmatic alteration. The samples display

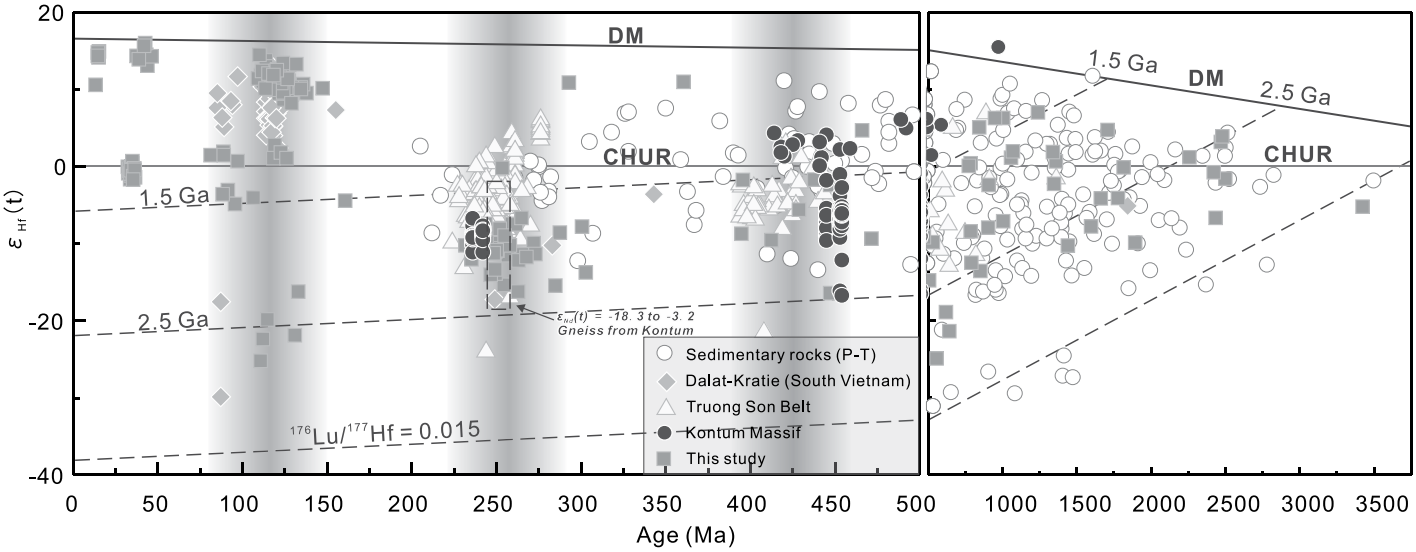

Figure 7. Zircon $\varepsilon_{Hf}(t)$ versus U-Pb age diagram for magmatic zircons from the Cebu and Bohol Islands and the eastern margin of Indochina block, including Truong Son Belt, Kontum Massif, and Dalat-Kratie, is shown. The detrital zircons from the Permian to Triassic sedimentary rocks of the Indochina block are also compiled for comparison. Hf isotope systematics for the Permian-Triassic zircons in this study are comparable to those for igneous rocks from the Kontum Massif in Eastern Indochina. Compiled Hf isotopic data and references are provided in Table S5 (see footnote 1) and cited from Shellnutt et al. (2013), Hieu et al. (2015), Arboit et al. (2016), Hieu et al. (2016), Wang et al. (2016), Hou et al. (2019), and Minh et al. (2020). The whole rock Nd isotopic compositions for the gneisses in the Kontum Massif are from Lan et al. (2003). DM—depleted mantle; CHUR—chondritic uniform reservoir.

no correlations between loss on ignition (LOI) with Rb, Ba, Sr and Th, and REEs (e.g., La, Yb) in Figure S6 (see footnote 1), indicating that their original signatures were not affected by post-magmatic alteration and the contents or ratios can be used to constrain the petrogenesis of the rocks sampled.

The high Mg# (42–71), low Rb/Sr and Rb/Ba ratios (0.002–0.085 and 0.023–0.221, respectively; Fig. 8A; Sylvester, 1998), and depleted whole rock Nd isotopic compositions ($\varepsilon_{Nd}(t) = +9.1$ to $+4.6$) collectively indicate that parental magmas of the igneous rocks in this study were dominated by mantle-derived basaltic melts. All samples are characterized by arc-like trace element patterns (Jagoutz and Kelemen, 2015) with depleted HFSEs (e.g., Nb, Ta, Ti) and enriched LILEs (e.g., Sr, Ba), indicating that subduction-related fluids/melts were involved in the magma source. These elemental and isotopic features indicate that the igneous rocks in the Cebu and Bohol Islands were formed in an arc or subduction-related setting. The low Th contents (0.1–5.2 ppm), low Th/Yb ratios (0.10–4.39), and variable Ba/La ratios (0.74–100.29) suggest a low sediment contribution to the magma source and that the arc-related rocks in this study were mainly derived from partial melting of the fluid-modified mantle wedge (Figs. 8B and 8C; Hawkesworth et al., 1997; Woodhead et al., 2001). The REE patterns for the late Eocene to early Oligocene andesite and basalt samples (B17, B19-1, and B20-2) from Bohol Island were more depleted than those of the average N-MORB (Fig. 3C); thus, we interpret that their basaltic parental magmas were from an ultra-depleted mantle affected by previous melt extraction, possibly the lithospheric mantle wedge and similar to the source of boninitic rocks (Chen et al., 2018). Conversely, the remaining samples from the Cebu and Bohol Islands were derived from asthenospheric or enriched lithospheric mantle wedge, the same as the source of typical arc rocks (Spandler and Pirard, 2013).

The identification of inherited/xenocrystic zircons with negative $\varepsilon_{Hf}(t)$ values in most samples suggests that continental materials were involved in the formation of the arc magmas. In addition, the presence of volcanic xenoliths (Fig. S1) in this study indicates that crustal assimilation occurred at shallow levels during the basaltic-andesitic magma ascent, which is consistent with the negative correlations between $\varepsilon_{Nd}(t)$ values and magma differentiation (Fig. 8D). Moreover, the simple binary mixing model between average Pacific N-MORB (Gale et al., 2013) and global subduction sediment (Plank and Langmuir, 1998) suggests that subducted sediment contaminant to the mantle wedge cannot generate the isotopic compositions of most samples studied (Fig. 9). Therefore, we propose that the Cretaceous to middle Miocene igneous rocks from the Cebu and Bohol Islands resulted from melting of a mantle wedge modified by subduction-related fluids with contamination by continental materials at crust levels rather than by source contamination.

Incorporation of Inherited/Xenocrystic Zircons and Implications for Continental Crustal Growth

Zircons from subducted sediments and rifted continental terranes may both be incorporated into arc magmatic rocks (Smyth et al., 2007; Shao et al., 2015; Rojas-Agramonte et al., 2016). But it is difficult to use conventional whole rock geochemical and isotopic criteria to distinguish the origin of inherited/xenocrystic zircons because subducted slab sediments and continental crust can share similar elemental or isotopic signatures (Plank and Langmuir, 1998; Buys et al., 2014). Conversely, if we know the source of the inherited/xenocrystic zircons, then the whole rock geochemistry of the source terrane can be used to test whether slab or continental crust components are involved in the incorporation of zircons. Nevertheless, the low contribution of sediments from the subducting slab to the petrogenesis and crustal contamination in shallow levels aforementioned indicate that inherited/xenocrystic zircons did not derive from the subducted sediments through slab melting. Therefore, the inherited/xenocrystic zircons were most likely incorporated into the arc rocks

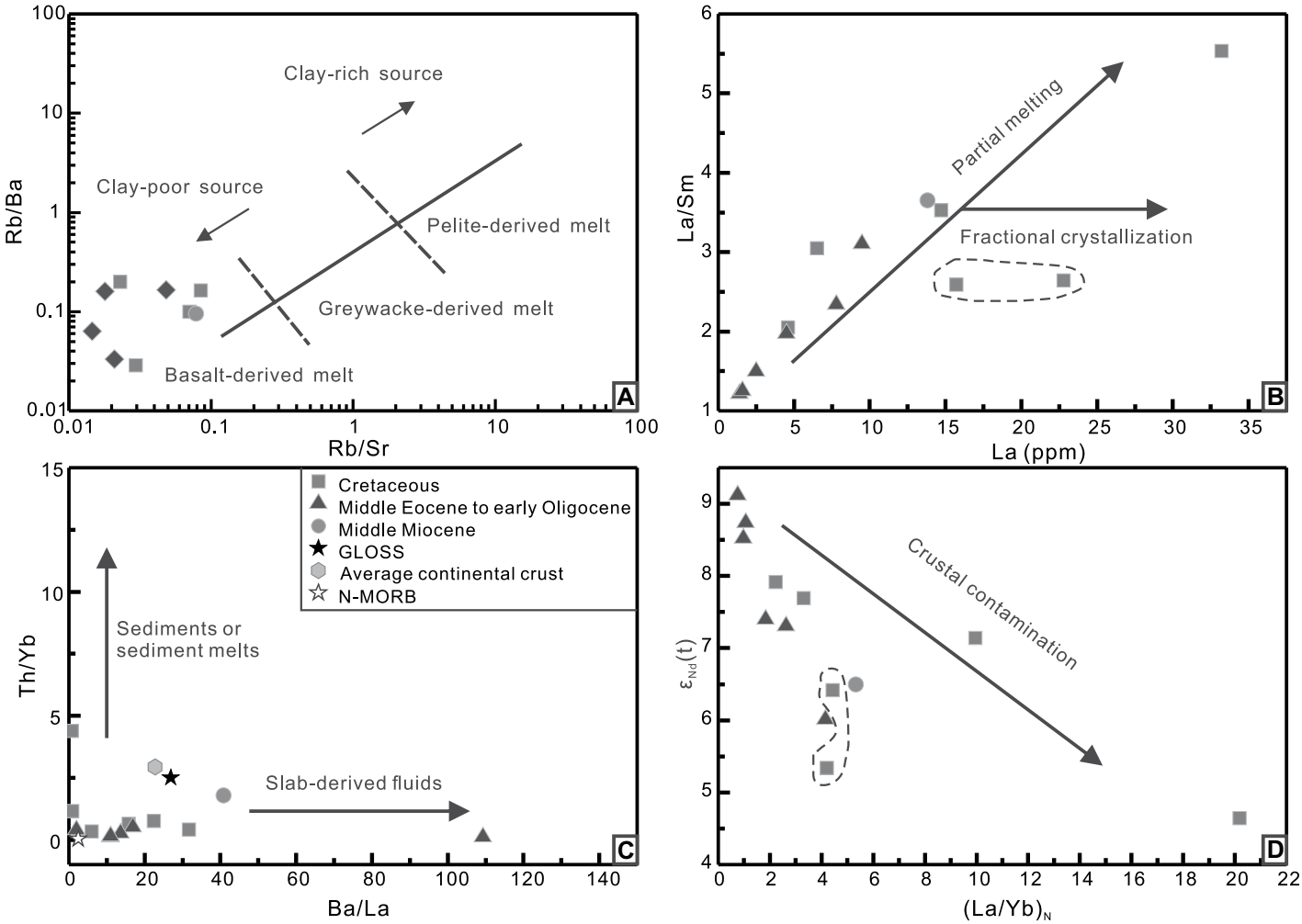

Figure 8. Diagrams show (A) Rb/Ba versus Rb/Sr (Sylvester, 1998), (B) La/Sm versus La, (C) Th/Yb versus Ba/La (Woodhead et al., 2001), and (D) $\varepsilon_{Nd}(t)$ versus $(La/Yb)_N$ for igneous rocks from the Cebu and Bohol Islands. Samples C15-1 and C17-1 are labeled with a dotted line in panels B and D. The $(La/Yb)_N$ represents the proxy for the degree of magmatic differentiation. The arrow shows the trend of differentiation in panel D, indicating that crustal contamination occurred in the shallow arc crust. Global subducting sediment (GLOSS), normal mid-oceanic-ridge basalt (N-MORB), and average continental crust compositions are from Plank and Langmuir (1998), Sun and McDonough (1989), and Rudnick and Gao (2003), respectively.

of this study from underlying intermediate-felsic crust and sedimentary cover during magma ascent and/or through remelting of underlying continental crust.

The Hf isotopic compositions of the Permian-Triassic zircons ($\varepsilon_{Hf}[t] = -16.2$ to -6.6) do not fall onto the continental evolution lines of the Cretaceous-Miocene grains (Fig. 7), indicating that these zircons were likely captured from Permian-Triassic granitoids with crustal model ages of 2.2–1.7 Ga or their eroded products during magma ascent. Conversely, some Cretaceous (ca. 126–81 Ma) and late Eocene to early Oligocene (ca. 36–32 Ma) zircons with low negative to low positive $\varepsilon_{Hf}(t)$ values of -4.9 to $+2.8$ and crust modal ages of ca. 1.5–1.0 Ga were possibly the product of melting of a common Mesoproterozoic continental crust during magma ascent rather than crystallized from a mixed source (i.e., mantle- and crust-derived melts). This is because large degrees of continental crust involvement were required to generate the zircon Hf isotopic systematics, and the mixing of mantle-derived magma with such significant involvement of crustal contamination is not possible in an island arc setting (at most 25% of granite or xenolith can be assimilated by mantle-derived basaltic magma to produce a hybrid magma; Glazner, 2007; Buys et al., 2014). Similarly, several Cretaceous zircons with high negative $\varepsilon_{Hf}(t)$ values of -25.2 to -16.2 may crystallize from the continental crust-derived melts with a crust model age of ca. 2.5 Ga. Although some of the Cretaceous to Paleogene zircons characterized by crust-like Hf isotopes were produced by melting of the continental crust, we infer that they were assimilated into the arc rocks by juvenile magmas with relatively younger ages than the crystallization age of these zircons based on the depleted whole rock Nd isotopes.

Island arcs are generally accepted to involve juvenile crustal materials with little or no contribution from continental crust (Buys et al., 2014). However, Paleogene, Cretaceous, and Permian-Triassic zircons in this study have negative $\varepsilon_{Hf}(t)$ values with Archean to Proterozoic crustal model (T_{DM}^{C}) ages (Fig. 7 and Table S4), which suggests that ancient continental crust was involved in the petrogenesis of the Philippine Mobile Belt arcs. Similar findings from other juvenile island arc crust, such as the Arabian-Nubian

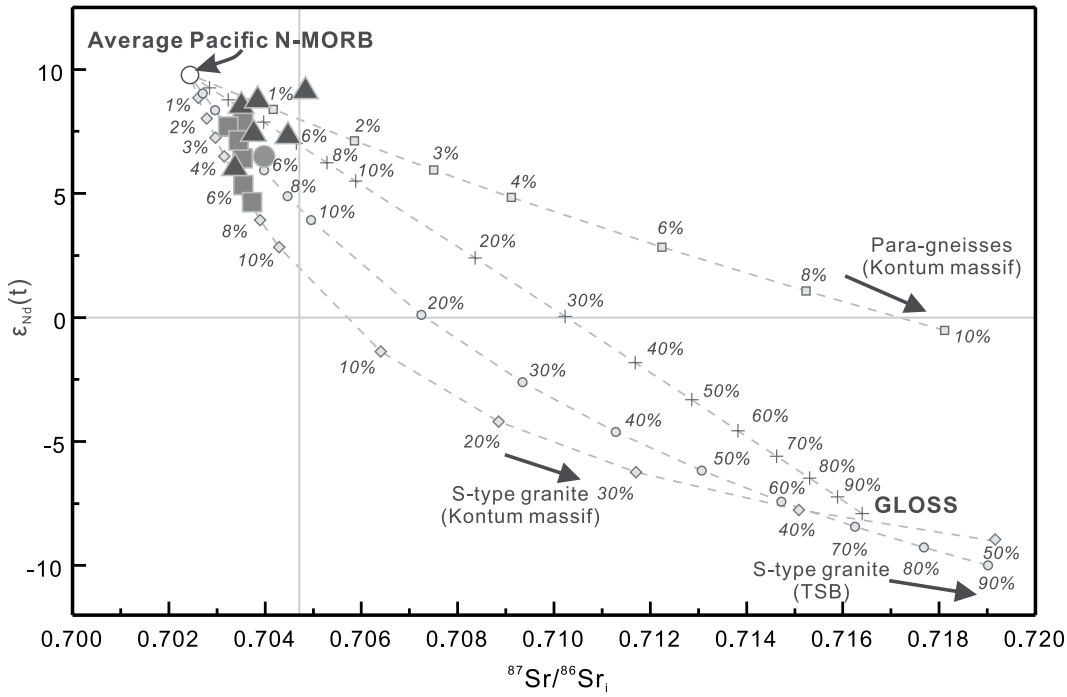

Figure 9. Diagram shows whole rock Sr versus Nd isotopic correlation for igneous rocks from the Cebu and Bohol Islands. Sources of data for comparison and modeling: the mean Pacific normal mid-oceanic-ridge basalt (N-MORB) (Gale et al., 2013), Sr = 111 ppm, Nd = 9.46 ppm, $^{87}Sr/^{86}Sr = 0.7024$, $\varepsilon_{Nd}(t) = 9.7$; global subducting sediment (GLOSS; Plank and Langmuir, 1998), Sr = 327 ppm, Nd = 27 ppm, $^{87}Sr/^{86}Sr = 0.7164$, $\varepsilon_{Nd}(t) = -7.9$; Permian-Triassic paragneisses in Kontum Massif (Lan et al., 2003), Sr = 237 ppm, Nd = 44.71 ppm, $^{87}Sr/^{86}Sr = 0.7842$, $\varepsilon_{Nd}(t) = -20.1$; Early Triassic S-type granite in Truong Son Belt (TSB; Thanh et al., 2019), Sr = 164 ppm, Nd = 34.1 ppm, $^{87}Sr/^{86}Sr = 0.7203$, $\varepsilon_{Nd}(t) = -10.6$; Permian-Triassic S-type granite in Kontum Massif (Hoa et al., 2008), Sr = 41 ppm, Nd = 40 ppm, $^{87}Sr/^{86}Sr = 0.7493$, $\varepsilon_{Nd}(t) = -11.9$. The Sr-Nd isotopic compositions of all end-members referred to in this study are corrected to ca. 125 Ma. Legends are the same as in Figure 8.

Shield (Hargrove et al., 2006; Li et al., 2018), the Vanuatu-Solomon arc (Buys et al., 2014; Tapster et al., 2014), the North Luzon arc (Shao et al., 2015), and the Caribbean arc (Kamenov et al., 2011), suggest that the incorporation of ancient continental materials into oceanic arcs may be more common than previously recognized.

Eastern Indochina Affinity of the Inherited/Xenocrystic Zircons

The Cretaceous (ca. 120–90 Ma), middle Eocene to early Oligocene (ca. 43–30 Ma), and middle Miocene (ca. 14 Ma) crystallization ages identified from the Cebu and Bohol Islands in this study are consistent with the presence of Mesozoic-Cenozoic magmatic arcs within the Philippine Mobile Belt (Aurelio and Peña, 2010; Deng et al., 2015); thus, the Cretaceous to middle Miocene zircons likely derived from these arc magmas through in situ crystallization. In contrast, the abundant Permian-Triassic inherited/xenocrystic zircons (Fig. 6A and Fig. S4), along with minor early Paleozoic to Archean zircons, likely originated from allochthonous terranes and may provide crucial clues regarding tectonic reconstructions. We hence follow the commonly used method of comparing the age distribution of zircons with tectonic and magmatic events from nearby exposed terranes (Rojas-Agramonte et al., 2016; Zhang et al., 2016, 2020a) to constrain the origin of the inherited/xenocrystic zircons. In addition, previous paleomagnetic data from Cebu Island were also used to assist in discriminating the origins (McCabe et al., 1987; Yumul et al., 2020a). We compiled zircon U-Pb ages and Hf isotopic data from surrounding terranes in which Permian-Triassic aged zircons/rocks have been reported, including the South China margin (Jiang et al., 2015; Shao et al., 2017), Palawan-Mindoro block (Suggate et al., 2014; Shao et al., 2017; Yan et al., 2018), Indochina-East Malaya block (Carter and Moss, 1999; Usuki et al., 2009; Shellnutt et al., 2013; Burrett et al., 2014; Tran et al., 2014; Hieu et al., 2015; Shi et al., 2015; Owada et al., 2016; Wang et al., 2016; Hennig et al., 2018; Dodd et al., 2019; Hou et al., 2019; Nguyen, 2019; Bui et al., 2020), Borneo (van Hattum et al., 2006; Galin et al., 2017; Hennig et al., 2017; Breitfeld and Hall, 2018; Hennig-Breitfeld et al., 2019), West Sulawesi (Hennig et al., 2016; Jaya et al., 2017), and the island of New Guinea (including Bird's Head, Bird's Neck, and Bird's Body) (Van Wyck and Williams, 2002; Webb et al., 2019; White et al., 2019).

The island of New Guinea, is the northern part of the Australian plate with Proterozoic-Paleozoic metamorphic basements intruded by Devonian-Carboniferous and Permian-Triassic granitoids (Jost et al., 2018; Webb et al., 2019). This is consistent with detrital zircon ages dominated by Paleoproterozoic-Mesoproterozoic (ca. 2.0–1.3 Ga), Devonian-Carboniferous (ca. 370–320 Ma), and Permian-Triassic populations from the metasedimentary and sedimentary rocks (Fig. 6D; Van Wyck and Williams, 2002; Decker et al., 2017; Webb et al., 2019; White et al., 2019). As Devonian-Carboniferous zircons are rare in our samples, and the paleolatitude of the igneous rocks in Cebu was in the northern hemisphere during the Cretaceous (McCabe et al., 1987; Yumul et al., 2020a), Bird's Head Peninsula, New Guinea, is unlikely to be the source of the Cretaceous and Permian-Triassic zircons in this study. The detrital or inherited zircon age spectra for the basement rocks from the West Sulawesi block are dominated by Mesoproterozoic, Triassic, and Cretaceous populations (Fig. 6E; Hennig et al., 2016; Jaya et al., 2017). These prominent Mesoproterozoic and Triassic peaks resemble those from Bird's Head; thus, previous studies have proposed that West Sulawesi block was close to Bird's Head (Hennig et al., 2016; Jaya et al., 2017; Zhang et al., 2020a). In contrast, the Cretaceous zircon population and the Jurassic grains from West Sulawesi were interpreted to derive from Borneo (Hennig et al., 2016). Given that Sulawesi was close to Bird's Head Peninsula during the Triassic and that Jurassic zircons are rare in our samples, we suggest that West Sulawesi is probably not the source of our inherited/xenocrystic zircons.

The Borneo and East Malaya blocks are both characterized by prominent Paleoproterozoic (ca. 1.85 Ga), Permian-Triassic, and Cretaceous zircons (Figs. 6F and 6G; Hall and Sevastjanova, 2012). Whereas the Permian-Triassic granitoids in East Malaya are dominated by I-type granite (Ng et al., 2015), the Hf isotopic compositions of the Permian-Triassic detrital zircons in East Malaya show that they crystallized from a mixed crust- and mantle-derived source (Sevastjanova et al., 2011; Dodd et al., 2019), and these are different from the negative $\varepsilon_{Hf}(t)$ values for the Permian-Triassic zircons in this study. Jurassic magmatism and detrital zircon populations have been reported in Borneo (Fig. 6F; Hennig-Breitfeld et al., 2019, and references therein), with Triassic arc-derived tonalites in northern Borneo having depleted zircon Hf isotopes (Burton-Johnson et al., 2020). These signatures are inconsistent with the samples studied, indicating that magmatic rocks or sedimentary rocks from Borneo and East Malaya are probably not the source of the inherited/xenocrystic zircons in the region studied. The Palawan-Mindoro block has been suggested to have rifted from the South China margin (Cathaysia block) during the spreading of the South China Sea since ca. 33 Ma (Yan et al., 2018, and references therein), and thus the Palawan-Mindoro block and the South China margin share comparable detrital zircon age patterns dominated by Jurassic-Cretaceous ages with some Triassic and Mesoproterozoic (ca. 1.85 Ga) populations (Figs. 6H and 6I; Suggate et al., 2014; Jiang et al., 2015; Shao et al., 2017; Yan et al., 2018). Jurassic zircons are rare in the Cebu and Bohol samples, and the Permian-Triassic zircons in the Palawan-Mindoro block display juvenile Hf isotopic compositions ($\varepsilon_{Hf}[t] = +4.3$ to $+14.4$; Walia and Knittel, 2018), whereas Hf isotopic compositions for the Cretaceous zircons from South China and the Palawan-Mindoro block are relatively more enriched than those of this study (Jiang et al., 2015; Yan et al., 2018), suggesting that they are unlikely to be the source of the zircons in this study.

The remaining potential source terrane is the Indochina block, which is characterized by thick Mesozoic (most in Early Cretaceous) continental red beds mainly exposed in the Khorat Plateau with Jurassic, Permian-Triassic, Ordovician-Silurian, and Proterozoic detrital zircon peaks (Fig. 6C; Carter and Moss, 1999; Burrett et al., 2014). The absence of Jurassic grains in the Cebu and Bohol samples may imply that Mesozoic sedimentary rocks in Indochina contribute little to the provenance. By contrast, the widespread Paleozoic-Mesozoic magmatic-metamorphic basements (including Truong Son Belt, Kontum, and Dalat-Kratie; Fig. 10) in the eastern margin of Indochina may represent the potential source terrane based on the comparable Permian-Triassic (peaking at ca. 250 Ma), Cretaceous, and minor Ordovician-Silurian zircon age populations (Fig. 6B) as well as the dominantly negative $\varepsilon_{Hf}(t)$ values for detrital zircons from modern river sediments in central Vietnam (Wang et al., 2018). The Hf isotopic compositions are relatively more depleted for the Permian-Triassic zircons in the Truong Son Belt (Wang et al., 2016; Hou et al., 2019) than those in this study, and the Cretaceous grains in Dalat-Kratie are not entirely comparable to the samples studied (Fig. 7; Shellnutt et al., 2013), but our data match well with the Permian-Triassic zircons of Kontum Massif (Hieu et al., 2015). We suggest that the source terrane (termed Eastern Indochina in this study) was likely an extension/part of the Kontum Massif on the eastern margin of Indochina during the Permian-Triassic and separated from the Dalat-Kratie region of south Vietnam before the Cretaceous.

In summary, the abundant Permian-Triassic zircon xenocrysts in this study were most likely to be derived during magma ascent through a continental terrane similar to the Kontum Massif in the eastern margin of Indochina. Nevertheless, further Hf isotopic data on Permian-Triassic and Cretaceous zircons from Borneo, south Vietnam, Sulawesi, and Bird's Head are still required to refine our interpretation. Using a simple binary mixing model with mean Pacific MORB (Gale et al., 2013) and S-type granite/para-gneisses in the Kontum Massif (Lan et al., 2003; Hoa et al., 2008), the degree of continental crust assimilation is estimated to 1%–8% in the petrogenesis of the igneous rocks from the Cebu and Bohol Islands (Fig. 9).

Implications for Tectonic Reconstruction

The new zircon data described above and the northern hemisphere paleolatitude during the Cretaceous (McCabe et al., 1987; Yumul et al., 2020a) suggest that the model proposing a link between the proto-Philippine Sea Plate and the northern margin of the Australia Plate (Pubellier et al., 2003; Zahirovic et al., 2014; Deng et al., 2015; Dimalanta et al., 2020) needs to be revised, and a new model involving a continental fragment with Eastern Indochina affinity is required to explain the formation of the Cebu and Bohol Islands (Fig. 8). This model may also offer insights into the evolution of the proto-South China Sea. Our model generally supports the reconstruction of Holloway (1982) regarding the origin of the Philippine arc system but based on more reliable age data in this study, an Early Cretaceous start to magmatism is proposed rather than the Late Cretaceous of Holloway (1982).

Previous studies suggested that the Late Triassic to Cretaceous magmatism in South China, SE Vietnam, and Borneo was related to the long-lived westward subduction of the Paleo-Pacific Plate, and that magmatic arcs formed an Andean-type continental margin (Shellnutt et al., 2013; Breitfeld et al., 2017; Hennig et al., 2017; Suo et al., 2019). However, our Cretaceous samples have relatively more depleted Nd-Hf isotopic compositions than those from SE Vietnam and South China (Shellnutt et al., 2013; Jiang et al., 2015; Yan et al., 2018), suggesting that the samples studied formed away from a continental margin. The only known Mesozoic oceanic basin between the Cebu and Bohol Islands and mainland Asia was the proto-South China Sea, but early models for the proto-South China Sea proposed that it was a gulf or part of the Paleo-Pacific Ocean after subduction ceased in the Late Cretaceous and situated between Indochina-South China in the north and Borneo in the south (Holloway, 1982; Taylor and Hayes, 1983; Hall and Breitfeld, 2017, and references therein). Alternatively, a younger proto-South China Sea triggered by back-arc extension during the Late Cretaceous to Eocene as result of eastward rollback of the Paleo-Pacific Plate has also been proposed (Morley, 2012; Zahirovic et al., 2014). Whereas these models questioned how the Eastern Indochina-derived fragment accreted to the Philippine Mobile Belt, we thus interpret that the proto-South China Sea was likely a back-arc extensional basin related to retreat of the subducting Meso/Neo-Tethys slab (Zhou et al., 2008; Sun, 2016) or Paleo-Pacific slab in the Late Jurassic to Early Cretaceous, and the continental fragment drifted from Eastern Indochina with the spreading of the proto-South China Sea. The eastward migration of the Jurassic to Cretaceous magmatic arc and emergence of Early Cretaceous extensional basins in South China have been proposed to result from slab roll back of the Paleo-Pacific Plate since the Early Cretaceous (ca. 135 Ma; Zhou and Li, 2000; Suo et al., 2019). Besides, within-plate or post-orogenic granites with ages of ca. 87 Ma identified in SE Vietnam (Shellnutt et al., 2013) indicate that extensional tectonic regime prevailed in the southeastern margin of Indochina. Such southwestward youngling of extension suggests that the proto-South China Sea was more likely linked to the eastward retreat of the subducting Paleo-Pacific slab from the earliest Cretaceous, which possibly triggered a continental fragment to drift away from Eastern Indochina (Fig. 11A). Similarly, the Zamboanga Peninsula possibly rifted from Cathaysia based on the assumption that it was part of the Palawan-Mindoro block (Yumul et al., 2004, and references therein).

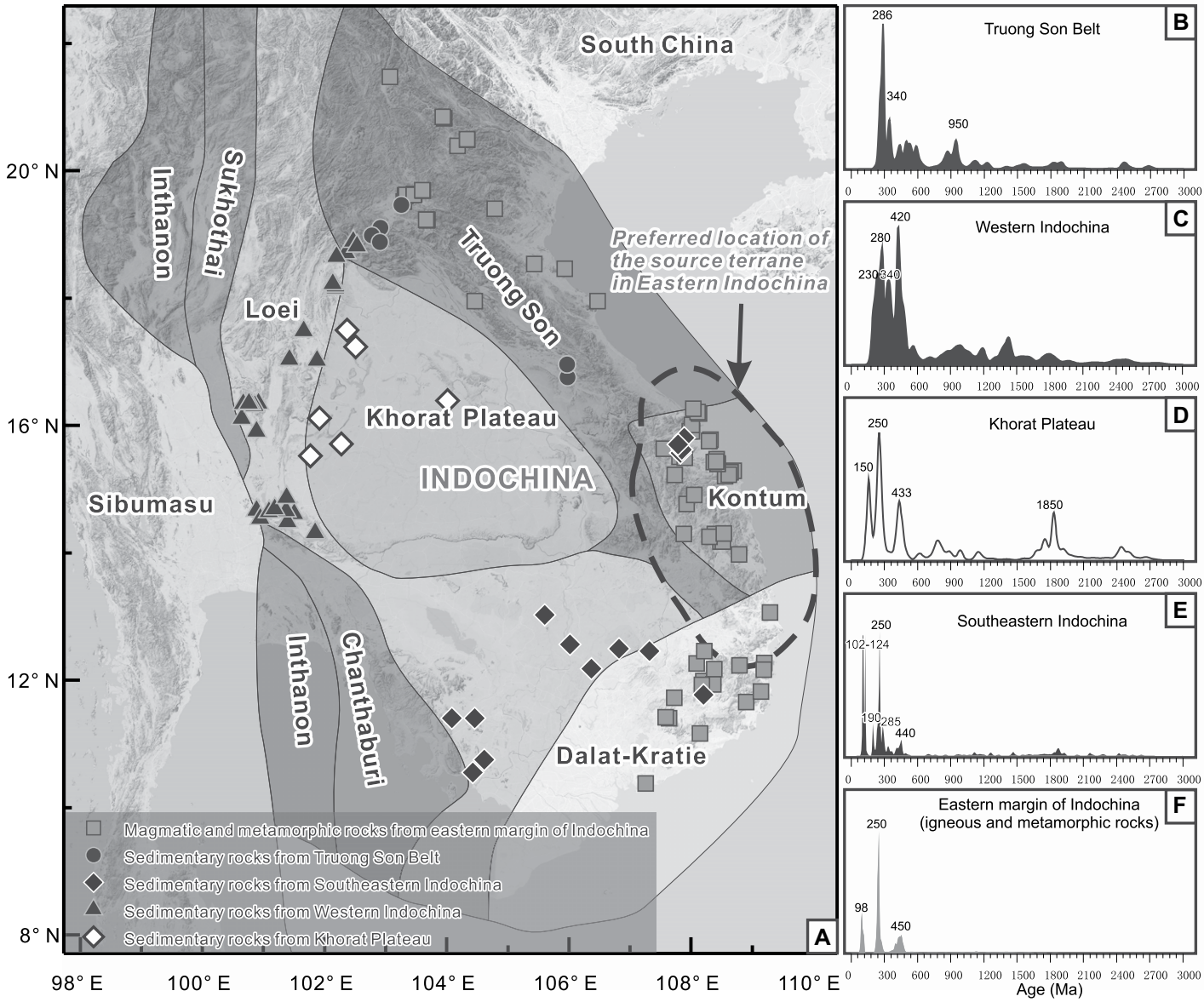

Figure 10. Distribution of the compiled samples from the Indochina block and the kernel density estimation spectra of the published zircon U-Pb ages from potential source terranes in Indochina is shown. The age distribution in panels B, C, D, and E are from sedimentary rocks, whereas in panel F is from igneous and metamorphic rocks. See Table S5 (see footnote 1) for compiled age data and references. GLOSS—global subducting sediment; TSB—Truong Son Belt.

The magmatic quiescence (ca. 80–50 Ma) in the Cebu and Bohol Islands possibly arose from slab shallowing and flat subduction that was similar to that observed in Sumatra (Zhang et al., 2019). Alternatively, no subduction during this time interval (Hall, 2012) resulted in magma termination. The young and buoyant Philippine Sea Plate migrated northward and was juxtaposed with the relatively older and denser proto-South China Sea at ca. 48 Ma, which resulted in the subduction of the proto-South China Sea beneath the Philippine Sea Plate (von Hagke et al., 2016). This subduction likely triggered the generation of the middle Eocene to early Oligocene (ca. 45–30 Ma) arc rocks on the Cebu and Bohol Islands (Fig. 11B), as suggested by seismic tomographic images across both islands (Wu et al., 2016; Fan et al., 2017). We suggest that this phase of arc magmatism formed part of the Cagayan arc based on the similar genesis of the samples studied and the Cagayan volcanic arc (Rangin, 1991). In addition, the subduction of the proto-South China Sea also possibly caused the formation of the Luzon arc (Hall, 2012). Meanwhile, continental fragments (e.g., Palawan) separated from the Cathysia block with the spreading of the South China Sea from ca. 33 Ma (Yan et al., 2018). Subduction of the proto-South China Sea ceased when the Reed Bank and Palawan-Mindoro block collided with the Cagayan arc in the early Miocene (Hall, 2013) and was followed by northward subduction of the Celebes Sea beneath the Cagayan arc to form the Sulu arc (Hall, 2013). Based on the rapid southeastward arc-trench rollback of the Sulu arc at ca. 16 Ma and extension of the Sulu Sea in the middle to late Miocene (Hall, 2013), we tentatively attribute the ca. 14 Ma andesite in Cebu Island to

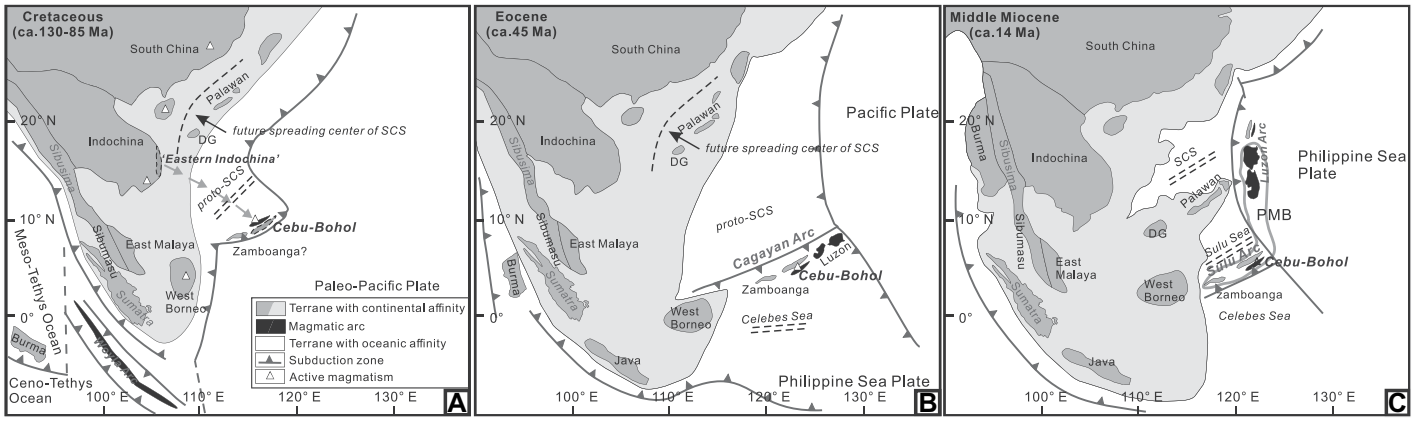

Figure 11. Tentative tectonic and paleogeographic reconstruction of Southeast Asia from Cretaceous to middle Miocene is shown. Positions of terranes are mainly modified from Hall (2012). The reconstruction for Burma is modified from Westerweel et al. (2019), Woyla arc is cited from Advokaat et al. (2018), Sibumasu (including Sibusima and Sumatra) is from Zhang et al. (2019), and the Sulu arc and Luzon arc are based on Hall (2013) and Shao et al. (2015), respectively. DG—dangerous grounds; SCS—South China Sea; PMB—Philippine Mobile Belt.

the southeastward rollback of the Celebes Sea, which moved the Cebu and Bohol Islands closer to the Philippine Mobile Belt (Fig. 11C). Based on the presence of the Permian-Triassic zircon population, this ca. 14 Ma andesitic magma passed through the pre-existing Eastern Indochina-derived fragment. Cathaysia-derived continental fragment accreted into the North Luzon arc in east Taiwan through similar processes (ca. 14 Ma; Shao et al., 2015).

CONCLUSIONS

Identification of abundant inherited/xenocrystic zircons from arc magmatic rocks from the Cebu and Bohol Islands indicates that ancient continental crust with Eastern Indochina affinity was recycled during the formation of juvenile arc magmas. This reinforces the importance of reworked ancient continental materials in the formation of intra-oceanic arcs. Our new data and tectonic model suggest that the Cretaceous arc in Cebu, the oldest arc within the Philippine Mobile Belt, was derived from the Eurasian margin rather than from the Australian margin as previously argued.

ACKNOWLEDGMENTS

We are grateful to the employees of the Carmen Copper Corporation and Regional Office 7, MGB, Philippines, for assistance with the field work. We also appreciate the constructive suggestions and comments of editor Rob Strachan, an anonymous reviewer, and Robert Hall and Xiaoran Zhang. This study was financially supported by the "135" Planned Project of Guangzhou Institute of Geochemistry, Chinese Academy of Sciences (135PY201606), the Strategic Priority Research Project (B) of the Chinese Academy of Sciences (XDB42000000), and Science and Technology Planning of Guangdong Province, China (2020B1212060055).

REFERENCES CITED

Advokaat, E.L., Bongers, M.L., Rudyawan, A., BouDagher-Fadel, M.K., Langereis, C.G., and van Hinsbergen, D.J., 2018, Early Cretaceous origin of the Woyla arc (Sumatra, Indonesia) on the Australian plate: Earth and Planetary Science Letters, v. 498, p. 348–361, https://doi.org/10.1016/j.epsl.2018.07.001.

Arboit, F., Collins, A.S., Morley, C.K., King, R., and Amrouch, K., 2016, Detrital zircon analysis of the southwest Indochina terrane, central Thailand: Unravelling the Indosinian orogeny: Geological Society of America Bulletin, v. 128, no. 5–6, p. 1024–1043, https://doi.org/10.1130/B31411.1.

Aurelio, M.A., and Peña, R.E., 2010, Geology of the Philippines, Second Edition: Quezon City, Philippines, Mines and Geosciences Bureau, Department of Environment and Natural Resources, 532 p.

Aurelio, M.A., Peña, R.E., and Taguibao, K.J.L., 2013, Sculpting the Philippine archipelago since the Cretaceous through rifting, oceanic spreading, subduction, obduction, collision and strike-slip faulting: Contribution to IGMA5000: Journal of Asian Earth Sciences, v. 72, p. 102–107, https://doi.org/10.1016/j.jseaes.2012.10.007.

Balmater, H.G., Manalo, P.C., Faustino-Eslava, D.V., Queaño, K.L., Dimalanta, C.B., Guotana, J.M.R., Ramos, N.T., Payot, B.D., and Yumul, G.P., 2015, Paleomagnetism of the Samar Ophiolite: Implications for the Cretaceous sub-equatorial position of the Philippine island arc: Tectonophysics, v. 664, p. 214–224, https://doi.org/10.1016/j.tecto.2015.09.024.

Blichert-Toft, J., and Albarède, F., 1997, The Lu-Hf isotope geochemistry of chondrites and the evolution of the mantle-crust system: Earth and Planetary Science Letters, v. 148, no. 1, p. 243–258, https://doi.org/10.1016/S0012-821X(97)00040-X.

Breitfeld, H.T., and Hall, R., 2018, The eastern Sundaland margin in the latest Cretaceous to Late Eocene: Sediment provenance and depositional setting of the Kuching and Sibu Zones of Borneo: Gondwana Research, v. 63, p. 34–64, https://doi.org/10.1016/j.gr.2018.06.001.

Breitfeld, H.T., Hall, R., Galin, T., Forster, M.A., and BouDagher-Fadel, M.K., 2017, A Triassic to Cretaceous Sundaland–Pacific subduction margin in West Sarawak, Borneo: Tectonophysics, v. 694, p. 35–56, https://doi.org/10.1016/j.tecto.2016.11.034.

Bui, V.T.S., Osanai, Y., Nakano, N., Adachi, T., Kitano, I., and Owada, M., 2020, Timing of high-grade metamorphism in the Kontum Massif, Vietnam: Constraints from zircon-monazite multi-geochronology and trace elements geochemistry of zircon-monazite-garnet: Journal of Asian Earth Sciences, v. 187, no. 104084, https://doi.org/10.1016/j.jseaes.2019.104084.

Burrett, C., Khin, Z., Meffre, S., Lai, C.K., Khositanont, S., Chaodumrong, P., Udchachon, M., Ekins, S., and Halpin, J., 2014, The configuration of Greater Gondwana—Evidence from LA ICPMS, U–Pb geochronology of detrital zircons from the Palaeozoic and Mesozoic of Southeast Asia and China: Gondwana Research, v. 26, no. 1, p. 31–51, https://doi.org/10.1016/j.gr.2013.05.020.

Burton-Johnson, A., Macpherson, C.G., Millar, I.L., Whitehouse, M.J., Ottley, C.J., and Nowell, G.M., 2020, A Triassic to Jurassic arc in north Borneo: Geochronology, geochemistry, and genesis of the Segama Valley Felsic Intrusions and the Sabah ophiolite: Gondwana Research, v. 84, p. 229–244, https://doi.org/10.1016/j.gr.2020.03.006.

Buys, J., Spandler, C., Holm, R.J., and Richards, S.W., 2014, Remnants of ancient Australia in Vanuatu: Implications for crustal evolution in island arcs and tectonic development of the southwest Pacific: Geology, v. 42, no. 11, p. 939–942, https://doi.org/10.1130/G36155.1.

Carter, A., and Moss, S.J., 1999, Combined detrital-zircon fission-track and U-Pb dating: A new approach to understanding hinterland evolution: Geology, v. 27, no. 3, p. 235–238, https://doi.org/10.1130/0091-7613(1999)027<0235:CDZFTA>2.3.CO;2.

Chen, M., Sun, M., Buslov, M.M., Cai, K., Jiang, Y., Kulikova, A.V., Zheng, J., and Xia, X., 2018, Variable slab-mantle interaction in a nascent Neoproterozoic arc–back-arc system generating boninitic-tholeiitic lavas and magnesian andesites: Geological Society of America Bulletin, v. 130, no. 9–10, p. 1562–1582, https://doi.org/10.1130/B31883.1.

Decker, J., Ferdian, F., Morton, A., Fanning, M., and White, L.T., 2017, New geochronology data from eastern Indonesia: An aid to understanding sedimentary provenance in a frontier region, *in* Proceedings, Indonesian Petroleum Association 41st Annual Convention: Jakarta, Indonesia, IPA17-551-G, p. 1–18.

Deng, J., Yang, X., Zhang, Z.F., and Santosh, M., 2015, Early Cretaceous arc volcanic suite in Cebu Island, Central Philippines and its implications on paleo-Pacific plate subduction: Constraints from geochemistry, zircon U–Pb geochronology and Lu-Hf isotopes: Lithos, v. 230, p. 166–179, https://doi.org/10.1016/j.lithos.2015.05.020.

Deng, J.H., Yang, X.Y., Qi, H.S., Zhang, Z.F., Mastoi, A.S., and Sun, W.D., 2017, Early Cretaceous high-Mg adakites associated with Cu-Au mineralization in the Cebu Island, Central Philippines: Implication for partial melting of the paleo-Pacific Plate: Ore Geology Reviews, v. 88, p. 251–269, https://doi.org/10.1016/j.oregeorev.2017.05.006.

Deschamps, A., and Lallemand, S., 2002, The West Philippine Basin: An Eocene to early Oligocene back arc

basin opened between two opposed subduction zones: Journal of Geophysical Research. Solid Earth, v. 107, no. B12, p. 2322, 10.1029/2001JB001706.

Dimalanta, C., Suerte, L., Yumul, G., Tamayo, R., and Ramos, E., 2006, A Cretaceous supra-subduction oceanic basin source for Central Philippine ophiolitic basement complexes: Geological and geophysical constraints: Geosciences Journal, v. 10, no. 3, p. 305–320, https://doi.org/10.1007/BF02910372.

Dimalanta, C.B., Faustino-Eslava, D.V., Gabo-Ratio, J.A.S., Marquez, E.J., Padrones, J.T., Payot, B.D., Queaño, K.L., Ramos, N.T., and Yumul, G.P., 2020, Characterization of the proto-Philippine Sea Plate: Evidence from the emplaced oceanic lithospheric fragments along eastern Philippines: Geoscience Frontiers, v. 11, no. 1, p. 3–21, https://doi.org/10.1016/j.gsf.2019.01.005.

Dodd, T.J.H., Gillespie, M.R., Leslie, A.G., Kearsey, T.I., Kendall, R.S., Bide, T.P., Dobbs, M.R., Millar, I.L., Lee, M.K.W., Chiam, K., and Goay, M., 2019, Paleozoic to Cenozoic sedimentary bedrock geology and lithostratigraphy of Singapore: Journal of Asian Earth Sciences, v. 180, no. 103878, https://doi.org/10.1016/j.jseaes.2019.103878.

Fan, J., Zhao, D., Dong, D., and Zhang, G., 2017, P-wave tomography of subduction zones around the central Philippines and its geodynamic implications: Journal of Asian Earth Sciences, v. 146, p. 76–89, https://doi.org/10.1016/j.jseaes.2017.05.015.

Fu, Y., Sun, X., Lin, H., Zhou, H., Li, X., Ouyang, X., Jiang, L., Shi, G., and Liang, Y., 2015, Geochronology of the giant Beiya gold-polymetallic deposit in Yunnan Province, Southwest China and its relationship with the petrogenesis of alkaline porphyry: Ore Geology Reviews, v. 71, p. 138–149, https://doi.org/10.1016/j.oregeorev.2015.05.016.

Fuller, M., McCabe, R., Williams, I.S., Almasco, J., Encina, R.Y., Zanoria, A.S., and Wolfe, J.A., 1983, Paleomagnetism of Luzon, *in* Hayes, D.E., ed., The Tectonic and Geologic Evolution of Southeast Asian Seas and Islands, Part 2: Washington, D.C., American Geophysical Union, Geophysical Monographs Series 27, p. 79–94, https://doi.org/10.1029/GM027p0079.

Fuller, M., Haston, R., and Almasco, J., 1989, Paleomagnetism of the Zambales ophiolite, Luzon, northern Philippines: Tectonophysics, v. 168, no. 1, p. 171–203, https://doi.org/10.1016/0040-1951(89)90375-2.

Fuller, M., Haston, R., Lin, J.-L., Richter, B., Schmidtke, E., and Almasco, J., 1991, Tertiary paleomagnetism of regions around the South China Sea: Journal of Southeast Asian Earth Sciences, v. 6, no. 3, p. 161–184, https://doi.org/10.1016/0743-9547(91)90065-6.

Gale, A., Dalton, C.A., Langmuir, C.H., Su, Y., and Schilling, J.G., 2013, The mean composition of ocean ridge basalts: Geochemistry, Geophysics, Geosystems, v. 14, no. 3, p. 489–518, https://doi.org/10.1029/2012GC004334.

Galin, T., Breitfeld, H.T., Hall, R., and Sevastjanova, I., 2017, Provenance of the Cretaceous-Eocene Rajang Group submarine fan, Sarawak, Malaysia from light and heavy mineral assemblages and U-Pb zircon geochronology: Gondwana Research, v. 51, p. 209–233, https://doi.org/10.1016/j.gr.2017.07.016.

Glazner, A.F., 2007, Thermal limitations on incorporation of wall rock into magma: Geology, v. 35, no. 4, p. 319–322, https://doi.org/10.1130/G23134A.1.

Griffin, W.L., Pearson, N.J., Belousova, E., Jackson, S.E., van Achterbergh, E., O'Reilly, S.Y., and Shee, S.R., 2000, The Hf isotope composition of cratonic mantle: LAM-MC-ICPMS analysis of zircon megacrysts in kimberlites: Geochimica et Cosmochimica Acta, v. 64, no. 1, p. 133–147, https://doi.org/10.1016/S0016-7037(99)00343-9.

Griffin, W.L., Wang, X., Jackson, S.E., Pearson, N.J., O'Reilly, S.Y., Xu, X., and Zhou, X., 2002, Zircon chemistry and magma mixing, SE China: In-situ analysis of Hf isotopes, Tonglu and Pingtan igneous complexes: Lithos, v. 61, no. 3, p. 237–269, https://doi.org/10.1016/S0024-4937(02)00082-8.

Grimes, C.B., John, B.E., Kelemen, P.B., Mazdab, F.K., Wooden, J.L., Cheadle, M.J., Hanghøj, K., and Schwartz, J.J., 2007, Trace element chemistry of zircons from oceanic crust: A method for distinguishing detrital zircon provenance: Geology, v. 35, no. 7, p. 643–646, https://doi.org/10.1130/G23603A.1.

Hall, R., 2002, Cenozoic geological and plate tectonic evolution of SE Asia and the SW Pacific: Computer-based reconstructions, model and animations: Journal of Asian Earth Sciences, v. 20, no. 4, p. 353–431, https://doi.org/10.1016/S1367-9120(01)00069-4.

Hall, R., 2012, Late Jurassic–Cenozoic reconstructions of the Indonesian region and the Indian Ocean: Tectonophysics, v. 570–571, p. 1–41, https://doi.org/10.1016/j.tecto.2012.04.021.

Hall, R., 2013, Contraction and extension in northern Borneo driven by subduction rollback: Journal of Asian Earth Sciences, v. 76, p. 399–411, https://doi.org/10.1016/j.jseaes.2013.04.010.

Hall, R., 2017, Southeast Asia: New views of the geology of the Malay Archipelago: Annual Review of Earth and Planetary Sciences, v. 45, no. 1, p. 331–358, https://doi.org/10.1146/annurev-earth-063016-020633.

Hall, R., and Breitfeld, H.T., 2017, Nature and demise of the Proto-South China Sea: Bulletin of the Geological Society of Malaysia, v. 63, p. 61–76, https://doi.org/10.7186/bgsm63201703.

Hall, R., and Sevastjanova, I., 2012, Australian crust in Indonesia: Australian Journal of Earth Sciences, v. 59, no. 6, p. 827–844, https://doi.org/10.1080/08120099.2012.692335.

Hall, R., Ali, J.R., Anderson, C.D., and Baker, S.J., 1995, Origin and motion history of the Philippine Sea Plate: Tectonophysics, v. 251, no. 1, p. 229–250, https://doi.org/10.1016/0040-1951(95)00038-0.

Hargrove, U.S., Stern, R.J., Kimura, J.I., Manton, W.I., and Johnson, P.R., 2006, How juvenile is the Arabian–Nubian Shield? Evidence from Nd isotopes and pre-Neoproterozoic inherited zircon in the Bi'r Umq suture zone, Saudi Arabia: Earth and Planetary Science Letters, v. 252, p. 308–326, https://doi.org/10.1016/j.epsl.2006.10.002.

Hawkesworth, C.J., Turner, S.P., McDermott, F., Peate, D.W., and van Calsteren, P., 1997, U-Th isotopes in arc magmas: Implications for element transfer from the subducted crust: Science, v. 276, no. 5312, p. 551, https://doi.org/10.1126/science.276.5312.551.

Hennig, J., Hall, R., and Armstrong, R.A., 2016, U-Pb zircon geochronology of rocks from west Central Sulawesi, Indonesia: Extension-related metamorphism and magmatism during the early stages of mountain building: Gondwana Research, v. 32, p. 41–63, https://doi.org/10.1016/j.gr.2014.12.012.

Hennig, J., Breitfeld, H.T., Hall, R., and Nugraha, A.M.S., 2017, The Mesozoic tectono-magmatic evolution at the Paleo-Pacific subduction zone in West Borneo: Gondwana Research, v. 48, p. 292–310, https://doi.org/10.1016/j.gr.2017.05.001.

Hennig, J., Breitfeld, H.T., Gough, A., Hall, R., Long, T.V., Kim, V.M., and Quang, S.D., 2018, U-Pb zircon ages and provenance of Upper Cenozoic sediments from the Da Lat Zone, SE Vietnam: Implications for an intra-Miocene unconformity and paleo-drainage of the Proto–Mekong River: Journal of Sedimentary Research, v. 88, no. 4, p. 495–515, https://doi.org/10.2110/jsr.2018.26.

Hennig-Breitfeld, J., Breitfeld, H.T., Hall, R., BouDagher-Fadel, M., and Thirlwall, M., 2019, A new upper Paleogene to Neogene stratigraphy for Sarawak and Labuan in northwestern Borneo: Paleogeography of the eastern Sundaland margin: Earth-Science Reviews, v. 190, p. 1–32, https://doi.org/10.1016/j.earscirev.2018.12.006.

Hieu, P.T., Yang, Y.Z., Binh, D.Q., Nguyen, T.B.T., Dung, L.T., and Chen, F., 2015, Late Permian to Early Triassic crustal evolution of the Kontum massif, central Vietnam: Zircon U-Pb ages and geochemical and Nd-Hf isotopic composition of the Hai Van granitoid complex: International Geology Review, v. 57, no. 15, p. 1877–1888, https://doi.org/10.1080/00206814.2015.1031194.

Hieu, P.T., Dung, N.T., Thuy, N.T.B., Minh, N.T., and Minh, P., 2016, U–Pb ages and Hf isotopic composition of zircon and bulk rock geochemistry of the Dai Loc granitoid complex in Kontum massif: Implications for early Paleozoic crustal evolution in Central Vietnam: Journal of Mineralogical and Petrological Sciences, v. 111, p. 326–336, https://doi.org/10.2465/jmps.151229.

Hoa, T.T., Anh, T.T., Phuong, N.T., Dung, P.T., Anh, T.V., Izokh, A.E., Borisenko, A.S., Lan, C.Y., Chung, S.L., and Lo, C.H., 2008, Permo-Triassic intermediate–felsic magmatism of the Truong Son belt, eastern margin of Indochina: Comptes Rendus Geoscience, v. 340, no. 2, p. 112–126, https://doi.org/10.1016/j.crte.2007.12.002.

Hoskin, P.W.O., and Schaltegger, U., 2003, The composition of zircon and igneous and metamorphic petrogenesis: Reviews in Mineralogy and Geochemistry, v. 53, no. 1, p. 27–62, https://doi.org/10.2113/0530027.

Holloway, N., 1982, North Palawan block, Philippines: Its relation to Asian mainland and role in evolution of South China Sea: American Association of Petroleum Geologists Bulletin, v. 66, no. 9, p. 1355–1383, https://doi.org/10.1306/03B5A7A5-16D1-11D7-8645000102C1865D.

Hou, L., Xiong, F., Wang, W., Guo, L., Peng, H., Ni, S., and Zhang, Q., 2019, Carboniferous-Triassic felsic igneous rocks and typical mineral deposits in the Truong Son orogenic belt, SE Asia: Implications for Paleo-Tethyan tectonic evolution and metallogeny: Ore Geology Reviews, v. 112, no. 103036, https://doi.org/10.1016/j.oregeorev.2019.103036.

Jackson, S.E., Pearson, N.J., Griffin, W.L., and Belousova, E.A., 2004, The application of laser ablation-inductively coupled plasma-mass spectrometry to in situ U-Pb zircon geochronology: Chemical Geology, v. 211, no. 1, p. 47–69, https://doi.org/10.1016/j.chemgeo.2004.06.017.

Jagoutz, O., and Kelemen, P.B., 2015, Role of arc processes in the formation of continental crust: Annual Review of Earth and Planetary Sciences, v. 43, no. 1, p. 363–404, https://doi.org/10.1146/annurev-earth-040809-152345.

Jaya, A., Nishikawa, O., and Hayasaka, Y., 2017, LA-ICP-MS zircon U-Pb and muscovite K-Ar ages of basement rocks from the south arm of Sulawesi, Indonesia: Lithos, v. 292–293, p. 96–110, https://doi.org/10.1016/j.lithos.2017.08.023.

Jiang, X.Y., Li, X.H., Collins, W.J., and Huang, H.Q., 2015, U-Pb age and Hf-O isotopes of detrital zircons from Hainan Island: Implications for Mesozoic subduction models: Lithos, v. 239, p. 60–70, https://doi.org/10.1016/j.lithos.2015.10.006.

Jochum, K.P., Nohl, U., Herwig, K., Lammel, E., Stoll, B., and Hofmann, A.W., 2005, GeoReM: A new geochemical database for reference materials and isotopic standards: Geostandards and Geoanalytical Research, v. 29, no. 3, p. 333–338, https://doi.org/10.1111/j.1751-908X.2005.tb00904.x.

Jost, B.M., Webb, M., and White, L.T., 2018, The Mesozoic and Palaeozoic granitoids of north-western New Guinea: Lithos, v. 312–313, p. 223–243, https://doi.org/10.1016/j.lithos.2018.04.027.

Kamenov, G.D., Perfit, M.R., Lewis, J.F., Goss, A.R., Arévalo, R., Jr., and Shuster, R.D., 2011, Ancient lithospheric source for Quaternary lavas in Hispaniola: Nature Geoscience, v. 4, p. 554–557, https://doi.org/10.1038/ngeo1203.

Lallemand, S., 2016, Philippine Sea Plate inception, evolution, and consumption with special emphasis on the early stages of Izu-Bonin-Mariana subduction: Progress in Earth and Planetary Science, v. 3, no. 1, p. 15, https://doi.org/10.1186/s40645-016-0085-6.

Lan, C.Y., Chung, S.L., Van Long, T., Lo, C.H., Lee, T.Y., Mertzman, S.A., and Shen, J.S., 2003, Geochemical and Sr-Nd isotopic constraints from the Kontum massif, central Vietnam on the crustal evolution of the Indochina block: Precambrian Research, v. 122, no. 1, p. 7–27, https://doi.org/10.1016/S0301-9268(02)00205-X.

Li, X.H., Leng, W.G., Li, Q.L., Liu, Y., Zheng, Y.F., Yang, Y.H., Chamberlain, K.R., Wan, D.F., Guo, C.H., Wang, X.C., and Tao, H., 2010, Penglai zircon megacrysts: A potential new working reference material for microbeam determination of Hf-O isotopes and U-Pb age: Geostandards and Geoanalytical Research, v. 34, no. 2, p. 117–134, https://doi.org/10.1111/j.1751-908X.2010.00036.x.

Li, X.H., Abd, E.R.Y., Abu, A.M., Li, J., Ling, X.X., Wu, L.G., and Masoud, A.E., 2018, Old continental crust underlying juvenile oceanic arc: Evidence from Northern Arabian-Nubian Shield, Egypt: Geophysical Research Letters, v. 45, no. 7, p. 3001–3008, https://doi.org/10.1002/2018GL077121.

Liang, X.R., Wei, G.J., Li, X.H., and Liu, Y., 2003, Precise determination of $^{143}Nd/^{144}Nd$ and Sm/Nd isotopes using MC-ICPMS: Geochimica, v. 32, p. 91–96.

Liu, Y., Hu, Z., Zong, K., Gao, C., Gao, S., Xu, J., and Chen, H., 2010, Reappraisement and refinement of zircon U-Pb isotope and trace element analyses by LA-ICP-MS: Chinese Science Bulletin, v. 55, no. 15, p. 1535–1546, https://doi.org/10.1007/s11434-010-3052-4.

McCabe, R., Kikawa, E., Cole, J.T., Malicse, A.J., Baldauf, P.E., Yumul, J., and Almasco, J., 1987, Paleomagnetic results from Luzon and the central Philippines: Journal of Geophysical Research: Solid Earth, v. 92, no. B1, p. 555–580, https://doi.org/10.1029/JB092iB01p00555.

Minh, N.T., Dung, N.T., Hung, D.D., Minh, P., Yu, Y., and Hieu, P.T., 2020, Zircon U-Pb ages, geochemistry and isotopic characteristics of the Chu Lai granitic pluton in the Kontum massif, central Vietnam: Mineralogy and Petrology, v. 114, no. 4, p. 289–303, https://doi.org/10.1007/s00710-020-00707-x.

Morley, C.K., 2012, Late Cretaceous-early Palaeogene tectonic development of SE Asia: Earth-Science Reviews, v. 115, no. 1, p. 37–75, https://doi.org/10.1016/j.earscirev.2012.08.002.

Ng, S.W.P., Whitehouse, M.J., Searle, M.P., Robb, L.J., Ghani, A.A., Chung, S.L., Oliver, G.J., Sone, M., Gardiner, N.J., and Roselee, M., 2015, Petrogenesis of Malaysian granitoids in the Southeast Asian tin belt: Part 2. U-Pb zircon geochronology and tectonic model: Geological Society of America Bulletin, v. 127, no. 9–10, p. 1238–1258, https://doi.org/10.1130/B31214.1.

Nguyen, H.H., 2019, The Cenozoic evolution of the South Vietnam margin of the South China Sea and the origin of coastal placer deposits [Ph.D. thesis]: London, University of London, 177 p.

Owada, M., Osanai, Y., Nakano, N., Adachi, T., Kitano, I., Van Tri, T., and Kagami, H., 2016, Late Permian plume-related magmatism and tectonothermal events in the Kontum Massif, central Vietnam: Journal of Mineralogical and Petrological Sciences, v. 111, no. 3, p. 181–195, https://doi.org/10.2465/jmps.151019b.

Pearce, J.A., 2014, Immobile element fingerprinting of ophiolites: Elements, v. 10, no. 2, p. 101–108, https://doi.org/10.2113/gselements.10.2.101.

Peccerillo, A., and Taylor, S.R., 1976, Geochemistry of Eocene calc-alkaline volcanic rocks from the Kastamonu area, Northern Turkey: Contributions to Mineralogy and Petrology, v. 58, no. 1, p. 63–81, https://doi.org/10.1007/BF00384745.

Plank, T., and Langmuir, C.H., 1998, The chemical composition of subducting sediment and its consequences for the crust and mantle: Chemical Geology, v. 145, no. 3, p. 325–394, https://doi.org/10.1016/S0009-2541(97)00150-2.

Pubellier, M., Ali, J., and Monnier, C., 2003, Cenozoic plate interaction of the Australia and Philippine Sea Plates: "Hit-and-run" tectonics: Tectonophysics, v. 363, no. 3, p. 181–199, https://doi.org/10.1016/S0040-1951(02)00671-6.

Queano, K.L., Ali, J.R., Milsom, J., Aitchison, J.C., and Pubellier, M., 2007, North Luzon and the Philippine Sea Plate motion model: Insights following paleomagnetic, structural, and age-dating investigations: Journal of Geophysical Research: Solid Earth, v. 112, no. B05101, https://doi.org/10.1029/2006jb004506.

Rangin, C., 1991, The Philippine Mobile Belt: A complex plate boundary: Journal of Southeast Asian Earth Sciences, v. 6, no. 3, p. 209–220, https://doi.org/10.1016/0743-9547(91)90068-9.

Rangin, C., Jolivet, L., and Pubellier, M., 1990, A simple model for the tectonic evolution of southeast Asia and Indonesia region for the past 43 m.y.: Bulletin de la Société Géologique de France, v. 6, no. 6, p. 889–905, https://doi.org/10.2113/gssgfbull.VI.6.889.

Rojas-Agramonte, Y., Garcia-Casco, A., Kemp, A., Kröner, A., Proenza, J.A., Lázaro, C., and Liu, D., 2016, Recycling and transport of continental material through the mantle wedge above subduction zones: A Caribbean example: Earth and Planetary Science Letters, v. 436, p. 93–107, https://doi.org/10.1016/j.epsl.2015.11.040.

Rudnick, R.L., and Gao, S., 2003, Composition of the continental crust: Treatise on Geochemistry, v. 3, p. 1–64, https://doi.org/10.1016/B0-08-043751-6/03016-4.

Sevastjanova, I., Clements, B., Hall, R., Belousova, E.A., Griffin, W.L., and Pearson, N., 2011, Granitic magmatism, basement ages, and provenance indicators in the Malay Peninsula: Insights from detrital zircon U–Pb and Hf-isotope data: Gondwana Research, v. 19, no. 4, p. 1024–1039, https://doi.org/10.1016/j.gr.2010.10.010.

Shao, L., Cao, L., Qiao, P., Zhang, X., Li, Q., and van Hinsbergen, D.J.J., 2017, Cretaceous–Eocene provenance connections between the Palawan Continental Terrane and the northern South China Sea margin: Earth and Planetary Science Letters, v. 477, p. 97–107, https://doi.org/10.1016/j.epsl.2017.08.019.

Shao, W.Y., Chung, S.L., Chen, W.S., Lee, H.Y., and Xie, L.W., 2015, Old continental zircons from a young oceanic arc, eastern Taiwan: Implications for Luzon subduction initiation and Asian accretionary orogeny: Geology, v. 43, no. 6, p. 479–482, https://doi.org/10.1130/G36499.1.

Shellnutt, J.G., Lan, C.Y., Van Long, T., Usuki, T., Yang, H.J., Mertzman, S.A., Iizuka, Y., Chung, S.L., Wang, K.L., and Hsu, W.Y., 2013, Formation of Cretaceous Cordilleran and post-orogenic granites and their microgranular enclaves from the Dalat zone, southern Vietnam: Tectonic implications for the evolution of Southeast Asia: Lithos, v. 182–183, p. 229–241, https://doi.org/10.1016/j.lithos.2013.09.016.

Shi, M.F., Lin, F.C., Fan, W.Y., Deng, Q., Cong, F., Tran, M.D., Zhu, H.P., and Wang, H., 2015, Zircon U–Pb ages and geochemistry of granitoids in the Truong Son terrane, Vietnam: Tectonic and metallogenic implications: Journal of Asian Earth Sciences, v. 101, p. 101–120, https://doi.org/10.1016/j.jseaes.2015.02.001.

Sláma, J., Košler, J., Condon, D.J., Crowley, J.L., Gerdes, A., Hanchar, J.M., Horstwood, M.S., Morris, G.A., Nasdala, L., and Norberg, N.J.C.G., 2008, Plešovice zircon—A new natural reference material for U-Pb and Hf isotopic microanalysis: Chemical Geology, v. 249, no. 1–2, p. 1–35, https://doi.org/10.1016/j.chemgeo.2007.11.005.

Smyth, H.R., Hamilton, P.J., Hall, R., and Kinny, P.D., 2007, The deep crust beneath island arcs: Inherited zircons reveal a Gondwana continental fragment beneath East Java, Indonesia: Earth and Planetary Science Letters, v. 258, no. 1, p. 269–282, https://doi.org/10.1016/j.epsl.2007.03.044.

Söderlund, U., Patchett, P.J., Vervoort, J.D., and Isachsen, C.E., 2004, The ^{176}Lu decay constant determined by Lu-Hf and U-Pb isotope systematics of Precambrian mafic intrusions: Earth and Planetary Science Letters, v. 219, no. 3, p. 311–324, https://doi.org/10.1016/S0012-821X(04)00012-3.

Spandler, C., and Pirard, C., 2013, Element recycling from subducting slabs to arc crust: A review: Lithos, v. 170–171, p. 208–223, https://doi.org/10.1016/j.lithos.2013.02.016.

Suggate, S.M., Cottam, M.A., Hall, R., Sevastjanova, I., Forster, M.A., White, L.T., Armstrong, R.A., Carter, A., and Mojares, E., 2014, South China continental margin signature for sandstones and granites from Palawan, Philippines: Gondwana Research, v. 26, no. 2, p. 699–718, https://doi.org/10.1016/j.gr.2013.07.006.

Sun, S.S., and McDonough, W.F., 1989, Chemical and isotopic systematics of oceanic basalts: Implications for mantle composition and processes, *in* Saunders, A.D., and Norry, M.J., eds., Magmatism in the Ocean Basins: Geological Society, London, Special Publication 42, no. 1, p. 313–345, https://doi.org/10.1144/GSL.SP.1989.042.01.19.

Sun, W., 2016, Initiation and evolution of the South China Sea: An overview: Acta Geochimica, v. 35, no. 3, p. 215–225, https://doi.org/10.1007/s11631-016-0110-x.

Suo, Y., Li, S., Jin, C., Zhang, Y., Zhou, J., Li, X., Wang, P., Liu, Z., Wang, X., and Somerville, I., 2019, Eastward tectonic migration and transition of the Jurassic-Cretaceous Andean-type continental margin along Southeast China: Earth-Science Reviews, v. 196, no. 102884, https://doi.org/10.1016/j.earscirev.2019.102884.

Sylvester, P.J., 1998, Post-collisional strongly peraluminous granites: Lithos, v. 45, no. 1, p. 29–44, https://doi.org/10.1016/S0024-4937(98)00024-3.

Tapster, S., Roberts, N.M.W., Petterson, M.G., Saunders, A.D., and Naden, J., 2014, From continent to intra-oceanic arc: Zircon xenocrysts record the crustal evolution of the Solomon island arc: Geology, v. 42, no. 12, p. 1087–1090, https://doi.org/10.1130/G36033.1.

Taylor, B., and Hayes, D.E., 1983, Origin and history of the South China Sea basin, *in* Hayes, D.E., ed., The Tectonic and Geologic Evolution of Southeast Asian Seas and Islands, Part 2: Washington, D.C., American Geophysical Union Geophysical Monograph Series, v. 27, p. 23–56, https://doi.org/10.1029/GM027p0023.

Thanh, T.V., Hieu, P.T., Minh, P., Nhuan, D.V., and Thuy, N.T.B., 2019, Late Permian-Triassic granitic rocks of Vietnam: The Muong Lat example: International Geology Review, v. 61, no. 15, p. 1823–1841, https://doi.org/10.1080/00206814.2018.1561335.

Tran, H.T., Zaw, K., Halpin, J.A., Manaka, T., Meffre, S., Lai, C.K., Lee, Y., Le, H.V., and Dinh, S., 2014, The Tam Ky-Phuoc Son Shear Zone in central Vietnam: Tectonic and metallogenic implications: Gondwana Research, v. 26, no. 1, p. 144–164, https://doi.org/10.1016/j.gr.2013.04.008.

Usuki, T., Lan, C.Y., Yui, T.F., Iizuka, Y., Van Vu, T., Tran, T.A., Okamoto, K., Wooden, J.L., and Liou, J.G., 2009, Early Paleozoic medium-pressure metamorphism in central Vietnam: Evidence from SHRIMP U-Pb zircon ages: Geosciences Journal, v. 13, no. 3, p. 245–256, https://doi.org/10.1007/s12303-009-0024-2.

van Hattum, M.W.A., Hall, R., Pickard, A.L., and Nichols, G.J., 2006, Southeast Asian sediments not from Asia: Provenance and geochronology of north Borneo sandstones: Geology, v. 34, no. 7, p. 589–592, https://doi.org/10.1130/G21939.1.

Van Wyck, N., and Williams, I.S., 2002, Age and provenance of basement metasediments from the Kubor and Bena Bena Blocks, central Highlands, Papua New Guinea: Constraints on the tectonic evolution of the northern Australian cratonic margin: Australian Journal of Earth Sciences, v. 49, no. 3, p. 565–577, https://doi.org/10.1046/j.1440-0952.2002.00938.x.

von Hagke, C., Philippon, M., Avouac, J.P., and Gurnis, M., 2016, Origin and time evolution of subduction polarity reversal from plate kinematics of Southeast Asia: Geology, v. 44, no. 8, p. 659–662, https://doi.org/10.1130/G37821.1.

Walia, M., and Knittel, U., 2018, Hf isotopes from Palawan Continental Terrane, Philippines—Clues to the evolution of sediment sources: Terrestrial, Atmospheric and Oceanic sciences journal, v. 29, no. 5, p. 523–534, https://doi.org/10.3319/TAO.2018.02.23.01.

Wang, C., Liang, X., Foster, D.A., Tong, C., Liu, P., Liang, X., and Zhang, L., 2018, Linking source and sink: Detrital zircon provenance record of drainage systems in Vietnam and the Yinggehai–Song Hong Basin, South China Sea: Geological Society of America Bulletin, v. 131, no. 1–2, p. 191–204, https://doi.org/10.1130/B32007.1.

Wang, S., Mo, Y., Wang, C., and Ye, P., 2016, Paleotethyan evolution of the Indochina Block as deduced from granites in northern Laos: Gondwana Research, v. 38, p. 183–196, https://doi.org/10.1016/j.gr.2015.11.011.

Webb, M., White, L.T., Jost, B.M., and Tiranda, H., 2019, The Tamrau Block of NW New Guinea records late Miocene-Pliocene collision at the northern tip of the Australian Plate: Journal of Asian Earth Sciences, v. 179, p. 238–260, https://doi.org/10.1016/j.jseaes.2019.04.020.

Wei, G., Liang, X., Li, X., and Liu, Y., 2002, Precise determination of Sr isotopes of solution and solid samples using (LP) MC-ICPMS: Geochimica, v. 31, p. 295–299.

Westerweel, J., Roperch, P., Licht, A., Dupont-Nivet, G., Win, Z., Poblete, F., Ruffet, G., Swe, H.H., Thi, M.K., and Aung, D.W., 2019, Burma Terrane part of the Trans-Tethyan arc during collision with India according to palaeomagnetic data: Nature Geoscience, v. 12, no. 10, p. 863–868, https://doi.org/10.1038/s41561-019-0443-2.

White, L.T., Hall, R., Gunawan, I., and Kohn, B., 2019, Tectonic mode switches recorded at the northern edge of the Australian Plate during the Pliocene and Pleistocene: Tectonics, v. 38, no. 1, p. 281–306, https://doi.org/10.1029/2018TC005177.

Wiedenbeck, M., Allé, P., Corfu, F., Griffin, W.L., Meier, M., Oberli, F., Quadt, A.V., Roddick, J.C., and Spiegel, W., 1995, The natural zircon standards for U-Th-Pb, Lu-Hf, trace element and REE analysis:

Geostandards Newsletter, v. 19, no. 1, p. 1–23, https://doi.org/10.1111/j.1751-908X.1995.tb00147.x.

Woodhead, J.D., Hergt, J.M., Davidson, J.P., and Eggins, S.M., 2001, Hafnium isotope evidence for 'conservative' element mobility during subduction zone processes: Earth and Planetary Science Letters, v. 192, no. 3, p. 331–346, https://doi.org/10.1016/S0012-821X(01)00453-8.

Wu, J., Suppe, J., Lu, R., and Kanda, R., 2016, Philippine Sea and East Asian plate tectonics since 52 Ma constrained by new subducted slab reconstruction methods: Journal of Geophysical Research: Solid Earth, v. 121, no. 6, p. 4670–4741, https://doi.org/10.1002/2016JB012923.

Wu, Y., and Zheng, Y., 2004, Genesis of zircon and its constraints on interpretation of U-Pb age: Chinese Science Bulletin, v. 49, no. 15, p. 1554–1569, https://doi.org/10.1007/BF03184122.

Yan, Y., Yao, D., Tian, Z., Huang, C., Chen, W., Santosh, M., Yumul, G.P., Jr., Dimalanta, C.B., and Li, Z., 2018, Zircon U-Pb chronology and Hf isotope from the Palawan-Mindoro Block, Philippines: Implication to provenance and tectonic evolution of the South China Sea: Tectonics, v. 37, no. 4, p. 1063–1076, https://doi.org/10.1002/2017TC004942.

Yuan, H.L., Gao, S., Dai, M.N., Zong, C.L., Günther, D., Fontaine, G.H., Liu, X.M., and Diwu, C., 2008, Simultaneous determinations of U-Pb age, Hf isotopes and trace element compositions of zircon by excimer laser-ablation quadrupole and multiple-collector ICP-MS: Chemical Geology, v. 247, no. 1, p. 100–118, https://doi.org/10.1016/j.chemgeo.2007.10.003.

Yumul, G., Jr., Zhou, M.F., Tamayo, R., Maury, R., Faustino, D., Olaguera, F., and Cotton, J., 2001, Onramping of cold oceanic lithosphere in a forearc setting: The Southeast Bohol Ophiolite Complex, Central Philippines: International Geology Review, v. 43, no. 9, p. 850–866, https://doi.org/10.1080/00206810109465052.

Yumul, G.P., Dimalanta, C.B., Tamayo, R.A., Maury, R.C., Bellon, H., Polvé, M., Maglambayan, V.B., Querubin, C.L., and Cotten, J., 2004, Geology of the Zamboanga Peninsula, Mindanao, Philippines: An enigmatic South China continental fragment?, *in* Malpas, J., Fletcher, C.J.N., Ali, J.R., and Aitchison, J.C., eds., Aspects of the Tectonic Evolution of China: Geological Society, London, Special Publication 226, no. 1, p. 289–312, https://doi.org/10.1144/GSL.SP.2004.226.01.16.

Yumul, G.P., Dimalanta, C.B., Maglambayan, V.B., and Marquez, E.J., 2008, Tectonic setting of a composite terrane: A review of the Philippine island arc system: Geosciences Journal, v. 12, no. 1, p. 7–17, https://doi.org/10.1007/s12303-008-0002-0.

Yumul, G.P., Dimalanta, C.B., Gabo-Ratio, J.A.S., Queaño, K.L., Armada, L.T., Padrones, J.T., Faustino-Eslava, D.V., Payot, B.D., and Marquez, E.J., 2020a, Mesozoic rock suites along western Philippines: Exposed proto-South China Sea fragments?: Journal of Asian Earth Sciences, v. X, no. 100031, https://doi.org/10.1016/j.jaesx.2020.100031.

Yumul, G.P., Dimalanta, C.B., Salapare, R.C., Queano, K.L., Faustino-Eslava, D.V., Marquez, E.J., Ramos, N.T., Payot, B.D., Guotana, J.M.R., Gabo-Ratio, J.A.S., Armada, L.T., Padrones, J.T., Ishida, K., and Suzuki, S., 2020b, Slab rollback and microcontinent subduction in the evolution of the Zambales Ophiolite Complex (Philippines): A review: Geoscience Frontiers, v. 11, no. 1, p. 23–36, https://doi.org/10.1016/j.gsf.2018.12.008.

Zahirovic, S., Seton, M., and Muller, R.D., 2014, The Cretaceous and Cenozoic tectonic evolution of Southeast Asia: Solid Earth, v. 5, no. 1, p. 227–273, https://doi.org/10.5194/se-5-227-2014.

Zhang, X., Zhao, G., Sun, M., Eizenhöfer, P.R., Han, Y., Hou, W., Liu, D., Wang, B., Liu, Q., and Xu, B., 2016, Tectonic evolution from subduction to arc-continent collision of the Junggar ocean: Constraints from U-Pb dating and Hf isotopes of detrital zircons from the North Tianshan belt, NW China: Geological Society of America Bulletin, v. 128, no. 3–4, p. 644–660, https://doi.org/10.1130/B31230.1.

Zhang, X., Chung, S.L., Lai, Y.M., Ghani, A.A., Murtadha, S., Lee, H.Y., and Hsu, C.C., 2018, Detrital zircons dismember Sibumasu in East Gondwana: Journal of Geophysical Research: Solid Earth, v. 123, no. 7, p. 6098–6110, https://doi.org/10.1029/2018JB015780.

Zhang, X., Chung, S.L., Hsu, C.C., Lai, Y.M., Ghani, A.A., and Murtadha, S., 2019, A 6000-km-long Neo-Tethyan arc system with coherent magmatic flare-ups and lulls in South Asia: Geology, v. 47, no. 6, p. 573–576, https://doi.org/10.1130/G46172.1.

Zhang, X., Tien, C.Y., Chung, S.L., Maulana, A., Mawaleda, M., Chu, M.F., and Lee, H.Y., 2020a, A late Miocene magmatic flare-up in West Sulawesi triggered by Banda slab rollback: Geological Society of America Bulletin, v. 132, https://doi.org/10.1130/B35534.1.

Zhang, Y., Tian, J., Hollings, P., Gong, L., Alburo, I., Berador, A.E., Francisco, D.G., Li, J., and Chen, H.Y., 2020b, Mesozoic porphyry Cu-Au mineralization and associated adakite-like magmatism in the Philippines: Insights from the giant Atlas deposit: Mineralium Deposita, v. 55, p. 881–900, https://doi.org/10.1007/s00126-019-00907-2.

Zhou, D., Sun, Z., Chen, H.Z., Xu, H.H., Wang, W.Y., Pang, X., Cai, D.S., and Hu, D.K., 2008, Mesozoic paleogeography and tectonic evolution of South China Sea and adjacent areas in the context of Tethyan and Paleo-Pacific interconnections: The Island Arc, v. 17, no. 2, p. 186–207, https://doi.org/10.1111/j.1440-1738.2008.00611.x.

Zhou, X.M., and Li, W.X., 2000, Origin of Late Mesozoic igneous rocks in Southeastern China: Implications for lithosphere subduction and underplating of mafic magmas: Tectonophysics, v. 326, no. 3, p. 269–287, https://doi.org/10.1016/S0040-1951(00)00120-7.

Science Editor: Rob Strachan
Associate Editor: Brian McConnell

Manuscript Received 15 June 2020
Revised Manuscript Received 28 October 2020
Manuscript Accepted 2 December 2020

Printed in the USA